Geological Society of America Bulletin

A nexus of plate interaction: Vertical deformation of Holocene wave-built terraces on the Kamchatsky Peninsula (Kamchatka, Russia)

Tatiana K. Pinegina, Joanne Bourgeois, Ekaterina A. Kravchunovskaya, Alexander V. Lander, Maria E.M. Arcos, Kevin Pedoja and Breanyn T. MacInnes

Geological Society of America Bulletin 2013;125, no. 9-10;1554-1568
doi: 10.1130/B30793.1

Notes

A nexus of plate interaction: Vertical deformation of Holocene wave-built terraces on the Kamchatsky Peninsula (Kamchatka, Russia)

Tatiana K. Pinegina[1,†], Joanne Bourgeois[2,†], Ekaterina A. Kravchunovskaya[3,§], Alexander V. Lander[4,†], Maria E.M. Arcos[5,†], Kevin Pedoja[6,†], and Breanyn T. MacInnes[7,†]

[1]*Institute of Volcanology and Seismology FED RAS, Petropavlovsk-Kamchatsky 683006, Russia*
[2]*Department of Earth and Space Sciences, University of Washington, Seattle, Washington 98195, USA*
[3]*Institute of Volcanology and Seismology FED RAS, Petropavlovsk-Kamchatsky 683006, Russia*
[4]*Institute of Earthquake Prediction Theory and Mathematical Geophysics RAS, Moscow 117997, Russia*
[5]*AMEC, 2101 Webster Street, Oakland, California 94612, USA*
[6]*UMR Centre National de la Recherche Scientifique 6143, "Morphodynamique Continentale et Côtière" (M2C), Université de Caen, 2-4 rue des Tilleuls, 14000 Caen, France*
[7]*Department of Geological Sciences, Central Washington University, Ellensburg, Washington 98926, USA*

ABSTRACT

Kamchatsky Peninsula lies within a complex meeting place of tectonic plates, in particular, the orthogonal interaction of the west-moving Komandorsky Island block with mainland Kamchatka. Examining the Holocene history of vertical deformation of marine wave-built terraces along the peninsular coast, we differentiated tectonic blocks undergoing uplift and tilting separated by zones of stable or subsided shorelines. We analyzed ~200 excavations along >30 coastal profiles and quantified vertical deformation on single profiles as well as along the coast using paleoshorelines dated with marker tephras. For the past ~2000 yr, the average rates of vertical deformation range from about –1 to +7 mm/yr. Uplift patterns are similar to those detected from historical leveling and from mapping of the stage 5e Quaternary marine terrace (ca. 120 ka). Average vertical deformation in the Holocene is highest for the shortest studied time period, from ca. A.D. 250 to 600, and it is several times faster than rates for marine oxygen isotope stage (MIS) 5e terraces. Vertical displacements observed along the coast are most likely coseismic and probably have included subsidence as well as uplift events. Because subsidence is generally associated with erosion, almost surely more prehistoric large earthquakes occurred than are recorded as topographic steps in these terraces. We suggest that the distribution of coastal uplift and subsidence observed along the Kamchatsky Peninsula coastline is qualitatively explained by the squeezing of the Kamchatsky Peninsula block between the Bering and Okhotsk plates, and the Komandorsky Island block.

INTRODUCTION

Geodynamic Setting

Among the promontories along the eastern coast of Kamchatka, the Kamchatsky Peninsula lies in the most complex tectonic setting (Fig. 1). It is difficult to find analogous places on the planet. While parts of Taiwan (Hsieh et al., 2004), Japan (Tamura et al., 2010), northern California (Merritts, 1996), and elsewhere are complex collisional, triple-junction, and multiplate locations, they have a smaller variety of geodynamic regimes over areas of the same spatial scale as the Kamchatsky Peninsula (~100 km length and 50 km width). The peninsula is situated at the northern terminus of the Kuril-Kamchatka subduction zone and where the Komandorsky Island block, moving parallel to the Aleutian trench, impinges on the Kamchatka mainland (Seliverstov, 1998, 2009). The region to the north of Kamchatsky Peninsula is interpreted to be the boundary between the Okhotsk and Bering plates (Lander et al., 1996; Mackey et al., 1997; Cross and Freymueller, 2008; Fig. 1).

The general explanation for the topographic expression of the Kamchatsky Peninsula is collision of the extinct Eocene Kronotsky island arc or the Aleutian-Komandorsky chain (at its western extent identified as the Komandorsky Island block) with the Kamchatka mainland (Geist and Scholl, 1994; McElfresh et al., 2002; Alexeiev et al., 2006; Lander and Shapiro, 2007; Scholl, 2007; Levin, 2009; Fig. 1), although some alternatives have been suggested (e.g., Kozhurin, 2007; for review, see Scholl, 2007,). Recent global positioning system (GPS) measurements show the Komandorsky Island block is moving west-northwest at a rate roughly half the rate of Pacific plate movement relative to Kamchatka (Fig. 1; Apel et al., 2006; Cross and Freymueller, 2008; Levin, 2009). However, we emphasize that the term "collision" in the context of Holocene tectonics may need qualification, in that the Komandorsky Island block is separated from Kamchatsky Peninsula by the >4000-m-deep Kamchatsky Strait, indicating thinner, if not oceanic, crust (Figs. 1B and 2). There is also the question of the mechanisms by which the strike-slip motions within and bounding the Komandorsky Island block are translated (or not) to the Kamchatsky Peninsula, and the way in which shear might be distributed between the Komandorsky Island block and the Kamchatka mainland. Other aspects of this region of nexus include the northwestern termination of the Pacific plate, as interpreted from seismic and geochemical data, and the northern termination of the active Kamchatka arc at Shiveluch volcano (Fig. 1; Levin et al., 2002; Park et al., 2002; Portnyagin et al., 2005).

Holocene Marine Terraces

Marine terraces record changes in relative sea level because their morphology is indicative of sea-level elevation at the time of terrace

†E-mails: pinegtk@yandex.ru (Pinegina); jbourgeo@uw.edu (Bourgeois, corresponding); land@mitp.ru (Lander); beth.arcos@amec.com (Arcos); kevin.pedoja@unicaen.fr (Pedoja); macinnes@geology.cwu.edu (MacInnes).
§Deceased 3 March 2013.

GSA Bulletin; September/October 2013; v. 125; no. 9/10; p. 1554–1568; doi: 10.1130/B30793.1; 7 figures; 2 tables; Data Repository item 2013301.

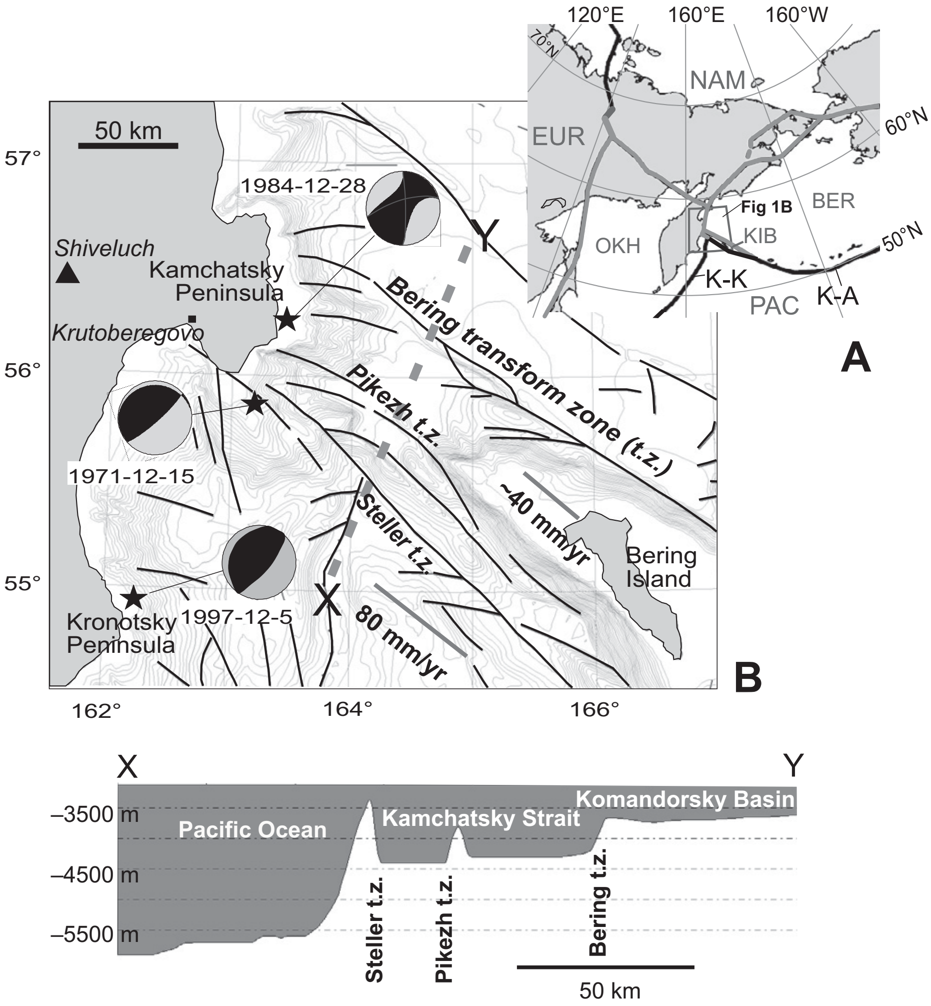

Figure 1. Tectonic setting of the Kamchatsky Peninsula. (A) Plate model for the NE Pacific region, adapted from Mackey et al. (1997) and Bourgeois et al. (2006). NAM—North American plate, EUR—Eurasian plate, PAC—Pacific plate, BER—Bering plate, OKH—Okhotsk plate, KIB—Komandorsky [Commander] Island block (McElfresh et al., 2002), K-A—Komandorsky-Aleutian trench, K-K—Kuril-Kamchatka Trench. Well-defined plate boundaries are shown in black; more diffuse boundaries are shown in gray. (B) Bathymetry (200 m contour interval) and major offshore faults near the Kamchatsky Peninsula (Seliverstov, 1998). The plate motion and three historical earthquakes shown are discussed in the text. Location of Shiveluch volcano is shown. Below: Profile X-Y, along X-Y line on 1B, showing depths of the Pacific Ocean, Kamchatsky Strait, and the Komandorsky Basin.

formation (Lajoie, 1986). The magnitude and rate of relative sea-level variation are major controls on the formation of marine terraces (wave-built or wave-cut), and on their height and morphology. Change in relative sea level is a product of regional or global sea-level rise and fall, and of more local vertical land movements such as from tectonic uplift or subsidence. In tectonically active areas, regional sea-level change over the late Holocene has been small relative to land-level changes (e.g., Chen and Liu, 2000); therefore, Holocene terraces can be distinct markers of neotectonic processes such as active faulting, tilting, intrusion and inflation, and vertical coseismic deformation.

Globally, more work has been conducted on Pleistocene marine terraces generated during interglacial, global highstands of sea level (review in Pedoja et al., 2011), than on uplifted Holocene marine terraces, which are typically restricted to areas of active tectonics (Lajoie, 1986). Moreover, most work on Holocene terraces has focused on wave-cut platforms and emergent coral reefs, rather than on the type of wave-built terraces (platforms) that are common in the Kamchatsky field area. Age control on Holocene marine terraces has been derived primarily from radiocarbon dating of associated faunal or plant material; a few studies have used optically stimulated luminescence dating (OSL; e.g., Bookhagen et al., 2006; Pflanz et al., 2013). The largest body of work on Holocene marine terraces has been carried out in the western Pacific (review by Ota and Yamaguchi, 2004), in particular in Japan (e.g., Sugihara et al., 2003; Ota and Yamaguchi, 2004; Tamura et al., 2010), Taiwan (e.g., Yamaguchi and Ota, 2002; Hsieh et al., 2004), New Zealand (Wilson et al., 2006; Berryman et al., 2011), and Papua New Guinea (e.g., Chappell et al., 1998). Other sites of study include Chile (Nelson and Manley, 1992; Bookhagen et al., 2006), the Mendocino triple junction (Merritts, 1996), and Indonesia (Vita-Finzi and Situmorang, 1989; Merritts et al., 1998; Briggs et al., 2008).

The coast of the Kamchatsky Peninsula in many places consists of flights of Pleistocene and Holocene terraces (Fig. 2; Pedoja et al., 2006, 2011). The shape of coastal cross-sectional profiles through these marine terraces depends on the rate and nature (gradual or discrete) of relative sea-level change. The "stair steps" of Holocene terraces here are sometimes separated by scarps from 0.5 m to several meters high (Fig. 2). Given that regional sea level has been essentially stable since 5000–6000 yr ago (Peltier, 2002; Woodroffe and Horton, 2005), we take the presence of these steps as evidence of rapid or abrupt uplift events during the Holocene. The steep erosional scarps indicate former episodes of coastal erosion, possibly due to relative sea-level rise during coastal subsidence. Thus, the morphology of the Holocene marine terraces of Kamchatsky Peninsula provides evidence of repeated high-amplitude (up to a few meters) changes in relative sea level during the past several thousand years.

The study of shoreline changes within Kamchatsky Peninsula is important because it can help elucidate the tectonic processes where Kamchatka and the Aleutian-Komandorsky chain interact. Several prior studies have examined both the instrumental (historic) and the Quaternary (10^5 yr) and longer time scales of tectonic movement of the Kamchatsky Peninsula; less attention has been paid to deformation on the Holocene time scale. The century to millennial scale of our work is long enough to manifest the main tendencies of Holocene tectonic deformation of Kamchatsky Peninsula blocks, but short enough to examine more specific questions such as: Are these vertical movements gradual or discrete, and are they unidirectional or alternating in their sense? How are the motions of active faults expressed topographically along the coast? This paper presents the results of our study of Holocene marine terraces, an approach that has been shown to be productive on other tectonically active margins (Chen and Liu, 2000; Hsieh et al., 2004; Bookhagen et al., 2006; Litchfield et al., 2010; Berryman et al., 2011).

PRIOR NEOTECTONIC OBSERVATIONS ON KAMCHATSKY PENINSULA

Instrumental Records

Seismicity

South of the Kamchatsky Peninsula, the subducting Pacific plate typically generates low-angle reverse-fault earthquakes in a Benioff-zone pattern, whereas on the Komandorsky segment of the Aleutian zone, right-lateral strike-slip earthquakes are prevalent (Gorbatov et al., 1997; Mackey et al., 2010). The seismicity of the junction area—the Kamchatsky Peninsula region—is neither Benioff zone nor transform, but is dominated by shallow, reverse and oblique-slip faulting. Thrusts with subhorizontal, NW-SE–oriented compression are prevalent, though there are a few normal-mechanism exceptions, for example, the earthquake of 27 August 2000 with Mb 4.9 (Global Centroid Moment Tensor Catalog, http://www.globalcmt.org/CMTsearch.html; see also Pinegina et al., 2010, their Fig. 7). Of note, the 15 December 1971 earthquake (Mw 7.8) (Fig. 1) and its aftershocks indicate oblique slip; the earthquake mechanism was thrust with a strike-slip component (Gusev and Zobin, 1975; Cormier, 1975; Okal and Talandier, 1986). The amount of slip calculated using seismic data was ~8 m, and the rupture produced a tsunami (Martin et al., 2008). The 28 December 1984 earthquake (Mw 6.7) (Fig. 1), occurring near Cape Africa, was originally interpreted by Fedotov et al. (1985) as strike slip with a minor thrust component. However, according to the Global Centroid Moment Tensor catalogue, it is not a clear double-couple mechanism and can be represented as a combination of E-W dextral strike slip and NW-SE compression, compensated linear-vector dipole (CLVD) tensor.

Leveling

On the Kamchatsky Peninsula, by repeat leveling along the coast in the period 1971–1986, Kirienko and Zolotarskaya (1989) established that average vertical movement rates were up to 10 mm/yr (Fig. 3). Leveling before and after the Mw 7.8 15 December 1971 earthquake measured relative vertical movement up to 80 mm of benchmarks situated on the coast (Levin et al., 2006). In 1972–1973, repeat measurement of relative elevations along the leveling lines from Cape Kamchatsky to Ust'-Kamchatsk (along the southern coast of the peninsula) and Pikezh River to Ozernoy Bay (eastern and northern coasts) showed that after the earthquake, the earth surface tilted to the NW (Kirienko and Zolotarskaya, 1989). Vertical deformation was also recorded in the 28 December 1984 earthquake; near Cape Africa, the relative vertical movement of benchmarks reached ~40 mm (Fig. 3).

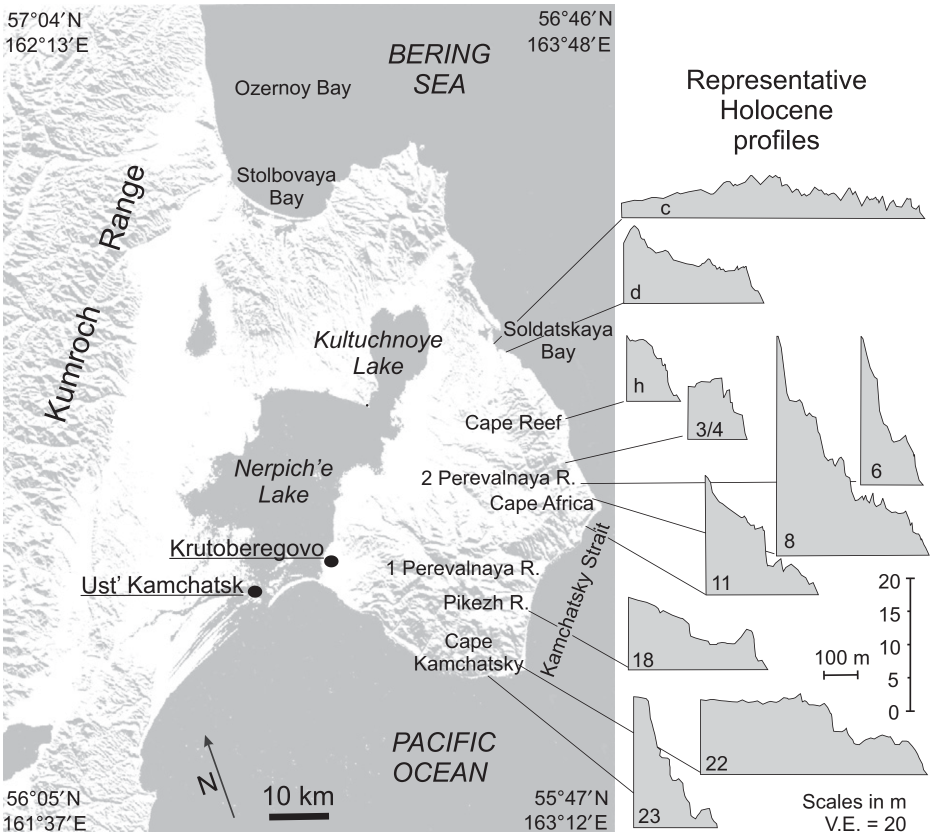

Figure 2. General topography based on digital elevation model (http://gs.mdacorporation.com/Mapping/DigitalElevationModels.aspx) of the Kamchatsky Peninsula region and examples of measured Holocene marine-terrace profiles along the outer coast of the Kamchatsky Peninsula (also see Fig. 1). The age of oldest terraces is 2000–4000 yr B.P. In all profiles, the shoreline is on the right side. Profile numbers are indicated in the lower-left corners. V.E.—vertical exaggeration.

Global Positioning Systems (GPS)

Since establishment of GPS instrumentation in the region (see Levin et al., 2006), no large earthquakes have occurred on or adjacent to the Kamchatsky Peninsula. However, the 1997 Kronotsky earthquake (December 5, Mw 7.8; see Fig. 1) did register coseismic and postseismic motion on nearby instruments at Krutoberegovo and on Bering Island (Bürgmann et al., 2005).

GPS measurements show that the Aleutian-Komandorsky chain is moving toward Kamchatka at a rate that increases to the west (Cross and Freymueller, 2008; Levin, 2009), with some indication of coupling with the Kamchatsky Peninsula. At the western end of the Komandorsky Island block, Bering Island moving ~35–50 mm/yr NW, relative to North America. On the western side of Kamchatsky Peninsula, Krutoberegovo is moving ~8–15 mm/yr (e.g., Bürgmann et al., 2005; Levin, 2009). However, because of the complex plate interactions of the region, and the short duration of the records, the deconvolution of GPS records into net plate motions is subject to interpretation (e.g., Apel et al., 2006; Kogan and Steblov, 2008).

Geomorphic and Geologic Analysis

Active Faults

Faults and structures connecting the Kamchatsky Peninsula to Komandorsky Island block transform faults have been proposed but

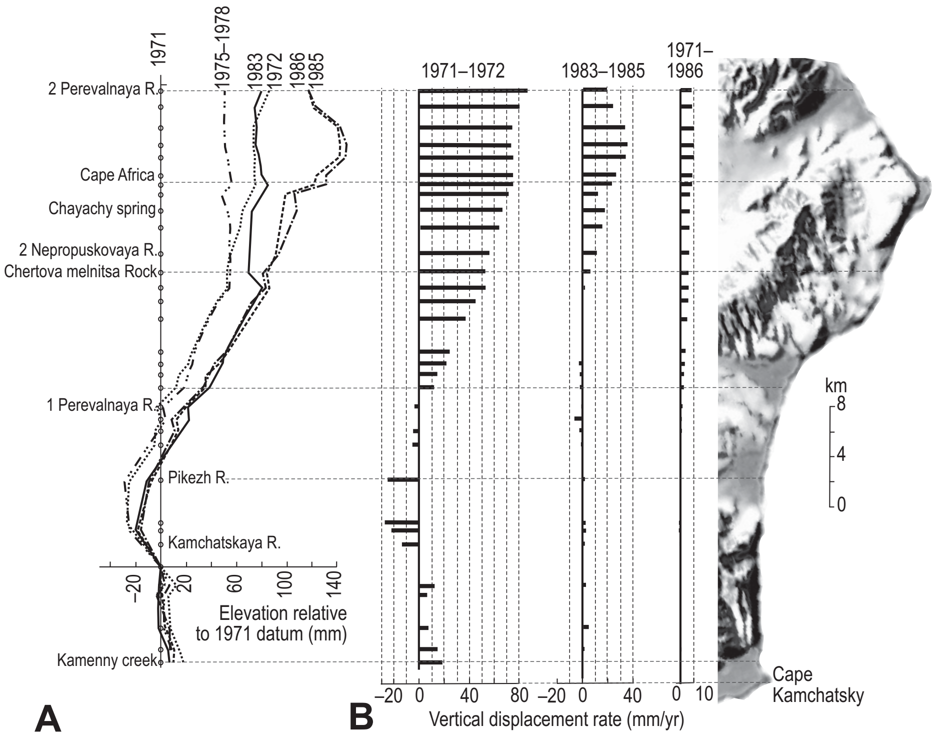

Figure 3. Measured, relative vertical displacements along the "Ust'-Kamchatsky testing area" (Kirienko and Zolotarskaya, 1989); the benchmark at Cape Kamchatsky was assigned a zero displacement. The leveling *y*-axis is distance along the coast, not latitude, so there is some variance—approximately lined up with the First and Second Pereval'naya Rivers mouths. (A) Vertical displacement graphs for the period A.D. 1971–1986. Measurement errors for the different years do not exceed ±8 mm (original plot by Kirienko and Zolotarskaya, 1989). (B) Calculated average of vertical motion (mm/yr) in the Ust'-Kamchatsky testing area for three time intervals: 1971–1972 and 1983–1985 (before and after the 1971 and 1984 earthquakes; see Fig. 1C and text), and the net rate, 1971–1986.

have not been mapped (Fig. 1). Gaedicke et al. (2000) and Freitag et al. (2001) suggested the continuation of transform faults associated with the Komandorsky block to structures within the Kamchatsky Peninsula. On the other hand, there is no geological or geophysical evidence of direct connections of Komandorsky Island block faults with the Kamchatsky Peninsula. Kozhurin (2007) trenched several faults on the peninsula and interpreted motions to be from clockwise rotation of the Kamchatsky Peninsula block caused by differential pressure of the impinging Komandorsky Island block, but he rejected a linkage of the faults to the offshore transform faults. Both groups have also analyzed aerial photographs of offset geomorphic features (e.g., Kozhurin, 2007; Baranov et al., 2010), with varying interpretations, discussed later herein.

Lineaments

In another methodological approach, McElfresh et al. (2002) used geographical information systems to examine the interaction of the Komandorsky Island block with Kamchatsky Peninsula. They analyzed clustering of linear features in the region and concluded that the patterns are best explained by the Komandorsky Island block moving rapidly toward Kamchatka, colliding and producing detectable lineaments represented on synthetic aperture radar (SAR) images in the Kamchatsky Peninsula. The age and activity of lineaments, however, are not well constrained, and air photos and our field work show that some of the lineaments are geomorphic features (for example, beach ridges, old shoreline angles).

Vertical Displacement

Uplift and exhumation rates on Kamchatsky Peninsula have been previously determined by mapping of Pleistocene terraces and by analysis of uplifted strata (Fedorenko, 1965; Erlikh et al., 1974; Freitag et al., 2001; Pedoja et al., 2006, 2011, 2013; Pflanz et al., 2013). According to Pleistocene terrace data, rates of coastal vertical movements on Kamchatsky Peninsula, averaged over a period of 120 k.y., range from 0.08 to 1.33 mm/yr (Pedoja et al., 2006). Based on apatite cooling ages, Freitag et al. (2001) reported exhumation rates in the later Cenozoic varying from 0.18 ± 0.04 mm/yr north of Cape Africa to 1.2 ± 0.18 mm/yr south of Cape Africa. Pflanz et al. (2013) determined recent uplift rates of coastal sediments by "remote sensing via ASTER and SRTM DEM combined with optically stimulated luminescence dating," where ASTER is the Advanced Spaceborne Thermal Emission and Reflection Radiometer and SRTM DEM is the Shuttle Radar Topography Mission digital elevation model. Pflanz et al.'s (2013) late Quaternary uplift rates via OSL vary from 0.8 to 7.5 mm/yr, and some results disagree with our analyses. A full evaluation of their work is beyond the scope of this paper; however, their analysis of a profile from Cape Africa (their Fig. 7) clearly disagrees with our analysis (see discussion presented in the Data Repository, including Fig. DR1[1]).

METHODS

Sea-Level Curve

Sea level is the datum by which we can reconstruct local vertical displacements, as long as we know the regional sea-level curve. A number of studies have generated sea-level curves for the Holocene of the northern Pacific (e.g., Selivanov, 1996a, 1996b; Douglas, 2001; Peltier, 2002; Woodroffe and Horton, 2005; Gehrels, 2010), the majority of which interpret a mid-Holocene sea-level highstand of 1–3 m from 5000 to 6000 yr B.P. and a return to approximately modern sea level from 4000 to 2000 yr B.P.

These model curves are in general agreement with our field studies, where we interpret that the Pacific Ocean–Bering Sea along the eastern coast of Kamchatka reached its maximal Holocene sea level at 5000–6000 yr B.P. (e.g., Pinegina et al., 2003, 2012; Bourgeois et al., 2006). This conclusion is based on multiple surveyed elevations of boundaries between coastal lagoon deposits and peat, dated using radiocarbon and tephra stratigraphy (Bourgeois et al., 2006; Pinegina et al., 2012). The mid-Holocene high and stabilization of sea level were followed by progradation of marine wave-built terraces along many Kamchatka coastlines. From consistency of beach ridge elevations on tectonically quiet Kamchatka coastlines (Martin et al.,

[1]GSA Data Repository item 2013301, Extended discussion, methods, Tables DR1 and DR2, Figures DR1–DR6, is available at http://www.geosociety.org/pubs/ft2013.htm or by request to editing@geosociety.org.

2004; Bourgeois et al., 2006; Pinegina et al., 2012), we interpret that since 5000–6000 yr ago, regional sea level has been stable within about ±1 m. For this reason, we interpret relative sea-level fluctuations along Kamchatsky Peninsula during the last ~5000 yr to have been caused primarily by coastal vertical tectonic deformation. This tectonic interpretation is supported by the significant (up to a few tens of meters) differences in elevation of Holocene marine terraces of the same age (based on tephra chronology) along the eastern coast of Kamchatka (this paper; Pedoja et al., 2006; Martin et al., 2004).

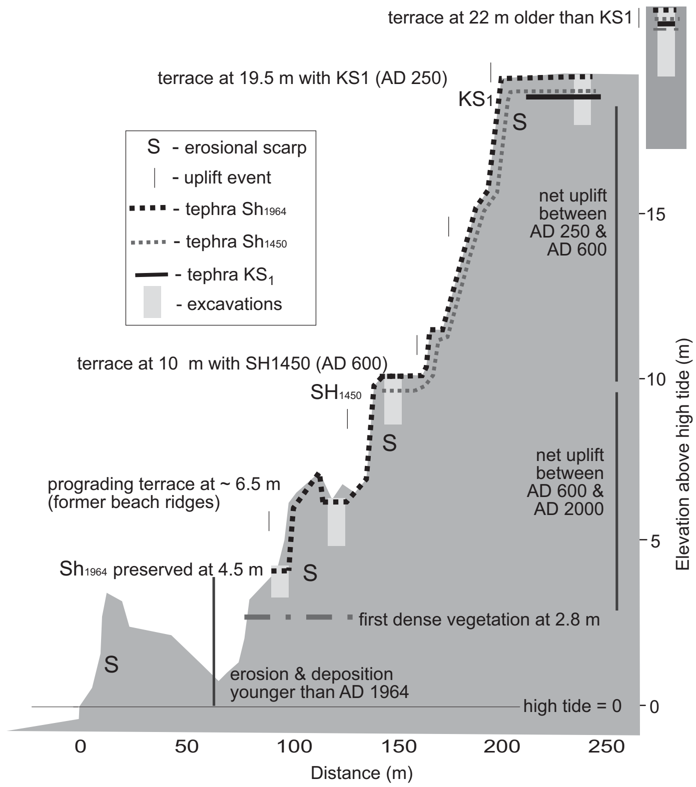

Figure 4. An example of a profile (profile 23) with very rapid net uplift. The profile is made of steep steps; steeper faces indicate cliff retreat and erosion. Tephras KS_1, Sh_{1450}, and Sh_{1964} are interpreted to be truncated by erosion, rather than pinching out (see Figs. 5 and 6). Additional profiles are shown in Figure DR1 (see text footnote 1).

Field Methods

During field seasons (primarily 2003 and 2004, with several profiles measured or remeasured in subsequent years), we measured 34 topographic profiles across wave-built marine terraces, composed typically of sand, but locally including granules and pebbles along the outer Kamchatsky Peninsula coast from Soldatskaya Bay to Kamchatsky Cape (Fig. 2). We also studied Holocene profiles from Stolbovaya Bay (Bourgeois et al., 2006), near Ust' Kamchatsk, and within the interior of Nerpich'e lake (Pinegina et al., 2012), all of which show subsidence to low rates of uplift during the later Holocene, with profiles preserving wave-built sequences of up to 6000 yr total. Most other parts of the Kamchatsky Peninsula coast are rocky cliffs, with lack of Holocene wave-built terraces, in some places even lacking present active beach deposits.

Along the 34 profiles, we dug multiple excavations (e.g., Fig. 4; Fig. DR2 [see footnote 1]), ~200 in all, typically 1 m to several meters deep. These excavations exposed soil-tephra sequences and beach (clean, well-sorted, gray sand) deposits, grading upward (and landward) from clean sand to a soil cap of weathered tephra and organic material. Coastal soils of these wave-built terraces can be assigned to Cryopsamments. The older the terrace, the thicker and more complex are the soil sequences, depending also on the rate of tephra deposition and the introduction of inorganic components (e.g., alluvium, colluvium, eolian sand). Most sequences are very sandy. In the field, we used such field terminology as "sandy soil" and "soily sand," where "sandy soil" had observable organic content, and "soily sand" showed only weathering (discoloration, silt component).

Our primary means for age control was tephra stratigraphy, not soil development. On Kamchatsky Peninsula, soil-pyroclastic cover, formed during the past 5000–6000 yr, contains up to 20 tephra layers (Bourgeois et al., 2006; Pinegina et al., 2012). In each excavation, we described and in some cases sampled these tephras, noting their position relative to soil development (Fig. 5A).

Age Control

We determined the age of raised terrace formation, i.e., the age when the surface was removed from the active shoreline, using the oldest marker tephra at the base of the soil sequence, directly above beach deposits. During an eruption, tephra falls can form distinctive marker horizons, which for Kamchatka have been mapped extensively over large areas (e.g., Braitseva et al., 1997). Marker tephras are chosen for having distinctive combinations of properties, from field characteristics such as color, grain size, thickness, and presence of pumice, to laboratory analyses of mineralogy and geochemistry. In this study, we used in particular the following marker tephras, which have been mapped in the study area and were distinctive in the field (Table 1; Pevzner et al., 1997; Bourgeois et al., 2006; Ponomareva et al., 2007; Pinegina et al., 2012): SH_{1964} (Shiveluch volcano, A.D. 1964 historical eruption), SH_{1450} (Shiveluch volcano, 1450 ^{14}C yr B.P. or ca. A.D. 600 eruption), and KS_1 (Ksudach volcano, 1800 ^{14}C yr B.P. or ca. A.D. 250 eruption).

The accuracy of tephra dating depends on the accuracy of ^{14}C dating of organic layers that underlie and overlie the tephra in key reference sections (e.g., Pevzner et al., 1997; Bourgeois et al., 2006). Since tephra layers have been dated using ^{14}C, the ages have ^{14}C-dating errors. These errors have been estimated based on error analysis of multiple dates for SH_{1450} (1400 ± 50 yr) and KS_1 (1750 ± 90 yr; references in Table 1). Herein we also provide a new, high-resolution date for an in-place woody shrub buried by KS_1 (in Soldatskaya Bay; Table 1; Table DR1 [see footnote 1]). Although there is error in ages assigned, because the tephras are time horizons, correlations between excavations and profiles are not affected by this error.

To distinguish air-fall (thus marker) tephra in excavations from redeposited tephra, we used the following criteria: each bed of air-fall tephra has a typical thickness, color, grain size, and internal stratigraphy, which correlate with its

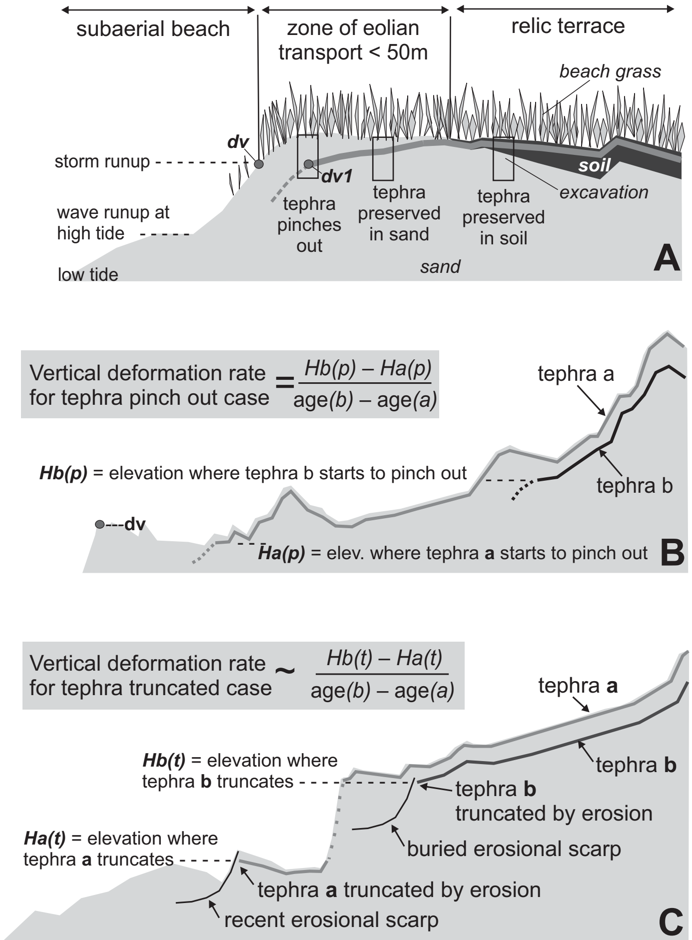

Figure 5. Method of determining the rate of vertical deformation between times of deposition of dated tephras on an accumulative coastal plain, using real profiles but with simplified stratigraphy. (A) Schematic geological section across a marine wave-built terrace (in the first months to several years after a tephra fall); *dv*—modern point of the dense vegetation; *dv1*—dense vegetation point by the time of tephra fall. (B) Simplified internal stratigraphy showing how comparable paleolocations (inflection where a tephra layer starts to pinch out) on the profile are measured and thus how a rate of vertical deformation is calculated. Note that from the elevation surveyed on the surface above Ha or Hb, we subtract the thickness of soil above the marker tephra being used, so the elevation is truly the elevation of the tephra when it was deposited on the surface. (C) Methods for calculating the rate of vertical deformation if there is a buried scarp. Example shows a real profile (profile 11, see Fig. 2). This profile exhibits two exposed erosional scarps—the labeled recent one (already partially buried), and the prominent cliff-like step (but there is no age control on this step). The profile also exhibits one buried erosional scarp, detected either by ground-penetrating radar or fortuitously by excavation. The "buried erosional scarp" is younger than tephra b and older than tephra a. The "recent erosional scarp" is younger than tephra a and older than sediments deposited on top of it. Buried scarps typically indicate a period or episode of subsidence (see text); however, this profile exhibits net uplift. The rate of net uplift is less accurately determined in this case than in part B, because the inflection point where the tephra starts to pinch out has been eroded away.

regionally mapped occurrence (e.g., Table 1). In addition, we looked for evidence of reworking, including admixture, redepositional textures, and rounding of soft pumiceous grains. In our reconstructions, we used two very well-traced prehistoric tephra layers. According to isopach maps, 1–5 cm of these tephras coated the Kamchatsky Peninsula (Bourgeois et al., 2006; Pinegina et al., 2012).

Measuring Relative Sea-Level Change (Uplift or Subsidence) on Accumulative Terraces

The standard method developed to measure relative sea-level change using marine terraces has been to identify the shoreline angle of uplifted or submerged wave-cut marine terraces, where the inflection point at the back of the terrace represents the base of a paleo–sea cliff (Lajoie, 1986; Burbank and Anderson, 2001; Keller and Pinter, 2002). In other regions of the world, specific coral and other organisms are used as markers relative to a sea-level datum (e.g., Sugihara et al., 2003). Along the Kamchatsky Peninsula, rather than erosion or coral growth, the Holocene shoreline has a history of net sand and soil accumulation, or aggradation. On these wave-built terraces composed of different ages of beach ridges, marker tephras are preserved, providing both good age control and reference elevation benchmarks relative to (paleo) sea level.

As previously noted, we assumed based on local and global sea-level studies that regional sea level was stable during the time span covered by of our study—the past 2000 yr. We also assumed that for each single profile location, the wave energy did not change significantly during the past 2000 yr. This is a weaker assumption, but it is supported by observations to the south of Ust' Kamchatsk (Fig. 2; Pinegina et al., 2012). At this site, sediment supply is large, and a wide (4–6 km) marine terrace composed of tens of beach ridges has accumulated during the past ~3000 yr, showing little difference in height or grain size for beach ridges formed during the past 2000 yr.

The method we used for reconstruction of paleoshorelines avoids error associated with variation of wave energy along the coast, and hence of beach-ridge height. Storm-beach height can also vary with sediment grain size, but the sand sizes in the terraces we studied remain consistently within the medium to coarse sand range. The energy of waves can vary over kilometers or less of distance due to differences in coastal exposure, nearshore bathymetry, etc. For example, on the outer Kamchatsky Peninsula coast, the elevation of the inland boundary of the

TABLE 1. HOLOCENE MARKER ASH LAYERS USED IN THIS STUDY, ON THE KAMCHATSKY PENINSULA, NE COAST OF KAMCHATKA, RUSSIA

Code	Source volcano	Age used in this study	Age (^{14}C yr B.P.)	Assigned calendar age	Characteristic features	Reference*	Field description	Thickness (cm)
SH_{1964}	Shiveluch	A.D. 1964 (historical)	Historical	A.D. 1964 (historical)	Medium K_2O content, high Cr and Sr content, presence of Hb, Ol	1*	White "salt and pepper" fine-medium sand	1–3
SH_{1450}	Shiveluch	A.D. 600	1450*	A.D. 540–640*	Medium K_2O content, high Cr and Sr content, presence of Hb	1*	Yellow "salt-and-pepper" fine to medium sand	1–3
KS_1	Ksudach	A.D. 250	1806 ± 16* *1850 ± 40*†	A.D. 160–340* *A.D. 71–249*†	Low K_2O content, absence of Hb	2* *This study*†	Pale yellow very fine to fine sand, some silt	3–7

Note: Tephra layers are listed in chronological order. In column 6, Hb—hornblende, Ol—olivine; other abbreviations are standard chemical symbols.
*Average of multiple dates; see (1) Pevzner et al. (1998); (2) Braitseva et al. (1997); also see Bourgeois et al. (2006).
†Single age, calibrated 2σ calendar age using CALIB 611 (Reimer et al., 2009); see Table DR1 (see text footnote 1).

active beach ranged from ~1.5 m to ~4.5 m (in most areas 2–3.5 m) above wave runup at high tide (marked by the highest recent flotsam). This factor means that we cannot correlate terraces along the coast by elevation alone, an issue also discussed and illustrated by Wilson et al. (2006) and McSaveney et al. (2006) for coastal areas of New Zealand.

Using these assumptions, and accounting for spatial wave-generated differences, we were able to compare elevations of terraces of different ages along the same profile and of the same age among profiles. In order to describe in detail our field-based approach, we would like first to discuss briefly a few important terms. Based on studies we have conducted on the Kamchatsky Peninsula and other coasts of Kamchatka in 1995–2012, it is possible to define three zones on marine wave-built terraces (Fig. 5A). Each of these zones is characterized by a particular regime of sedimentation (from shore toward land):

1. The subaerial beach is regularly affected by waves, resulting in intensive sediment erosion and redeposition. The beach is usually significantly steeper than the terrace above it. The modern upper boundary of the subaerial beach is marked by vegetation. We observe that sparse pioneer plants (such as *Honckenya oblongifolia*, *Mertensia maritima*) grow over several years on the upper part of the subaerial beach, which is inundated only during the strongest storms.

2. The zone of eolian transport is landward from the active beach, which can also include storm washover or splash-over deposits. The thickness of the layer affected by wind is generally ≤1 m and becomes thinner landward. Based on analysis of all profiles from Kamchatsky Peninsula, the zone of eolian transport along the peninsula is <50 m wide. It is typically dominated by beach rye grass (*Leymus mollis*), with increasingly dense and diverse vegetation landward, including also *Lathyrus japonicus*, *Senecio pseudoarnica*, *Lagedium sibiricum*, *Poa macrocalyx*, and *Trientalis europaea* subsp. *arctica*.

3. The relic terrace is landward of the zone of eolian transport and continues to the Holocene shoreline angle (the intersection of the Holocene marine terrace with a relic sea cliff). Eolian processes here are weak enough that soil can form. Beach rye cedes to other vegetation noted already and additional grasses, flowers, and low shrubs. Sedimentation rates are low compared to the subaerial beach and zone of eolian transport.

Tephra delineates the part of a (relic) terrace that already existed at the time of tephra fall. Preservation of tephra on a marine wave-built terrace depends on the sedimentation regime. On the relic terrace and in the zone of eolian transport, tephras can be well preserved. On the relic terrace, they are covered afterward by newly formed soil (or sandy soil, or soily sand, if close to the zone of eolian transport). In the zone of eolian transport, they are covered by sand, up to ~1 m thick (Fig. 5A). On upper subaerial beach, tephras can be preserved, but usually only as rewashed fragments or in lenses. In the lower subaerial beach, as well as underwater, tephras are redistributed by waves, and distinct layers are not preserved.

By studying buried tephras on marine wave-built terraces, it is possible to estimate the position of all three zones at the time of tephra fall. Tracing a buried tephra horizon from the land seaward, first we see it lying above a thin (young) soil, indicating the relic terrace formed by the time of tephra fall. Seaward, the tephra gradually deepens in soil and sand relative to the modern surface. The thickness of clean sand above the tephra increases up to ~1 m in the zone of eolian transport in the years following the tephra fall. Seaward of the zone of eolian transport, the tephra becomes deeper in clean sand at a very steep dip angle, close to the angle of the modern beach. This zone indicates the upper part of the subaerial beach at the time of tephra fall. The inflection point in the trend of tephra depth corresponds to the upper boundary of the subaerial beach at the time of tephra fall.

In order to determine the change in land level relative to the sea, in each excavation we tied our observation to a reference relative to modern wave action and sea level, for which we used the point of the first growth of dense vegetation (dv, Fig. 5). We measured and marked this point on all our modern profiles and associated this point in excavations with good preservation of tephra layers.

Seaward from the land, tephra layers in excavations pinch out in two ways: gradually (deposited during the terrace progradation; Figs. 5A and 5B) or abruptly (truncated by erosion; Fig. 5C). In the gradual pinch-out case, a tephra begins to dip seaward toward the shoreline, to appear deeper and in clean-sand deposits, and then to disappear. We identified the point on the profile where a tephra started to incline more steeply seaward and used this to indicate the seaward limit of dense vegetation (dv1) at the time the tephra was deposited (Ha[p] and Hb[p] on Fig. 5B). The deeper tephra in clean sand we interpreted to have been deposited on the upper, sparsely vegetated beach, as in Figure 5A. Consequently, the elevation above sea level of Ha(p) and Hb(p) at the moment of ash fall was equivalent to the modern elevation dv (Fig. 5B). The difference between Ha(p) and Hb(p) is the amount of uplift between the two times of tephra deposition, and the rate of uplift is that difference divided by the difference in tephra ages.

In the second case (Fig. 5C), a tephra is truncated abruptly by erosion during sea-level rise and landward scarp retreat. The unconformity created by scarp erosion means we do not know the position of the paleoshoreline when the tephra fell. We can only determine that the beach ridge closest to the sea where we still find the tephra is older than this tephra, so calculation of the amount of uplift is more approximate. In areas where tephras are cut out abruptly, quite often there is a significant age difference between two nearest beach ridges. This unconformity is either reflected in terrace morphology or in a buried erosional scarp (Fig. 5C). Where it was obvious that parts of the terrace and overlying tephra(s) were reworked, ages and thus rates of vertical deformation are approximate. Table 2 summarizes our calculations, with error, which is discussed in more detail in the Data Repository (DR2 [see footnote 1]).

The level of detail in reconstructing marine terrace history depends not only on tephra (and thus paleosurface) preservation, but also on the frequency of tephra falls, and the precision of their age determination. In this study, although up to five additional tephras for the past ~2000 yr exist, we used only the two most certain marker tephra and the modern surface to determine rates of Holocene vertical deformation for three time intervals (Table 2; DR2 [see footnote 1]): A.D. 250–2000, A.D. 600–2000, and A.D. 250–600, using rounded calendar ages for modern (A.D. 2000), SH_{1450} (A.D. 600), and KS_1 (A.D. 250) ages. In areas where part of a terrace (we presume) formed during a chosen time interval but was completely eroded, as indicated by missing tephra, the rate of deformation was not determined for that interval. In our calculations, we did not use Shiveluch tephra from the A.D. 1964 eruption, but we traced this horizon in excavations near the modern shoreline, using its patterns of bedding and pinching out to help us understand the characteristics of the zone of eolian transport (width, depth) and distribution of older tephra and to help identify the aggradation and erosion processes that have dominated beach profiles over the last few decades.

RESULTS: HOLOCENE VERTICAL DEFORMATION ON THE KAMCHATSKY PENINSULA COAST FROM RECONSTRUCTED PALEOSHORELINES

Tectonic movement, as expressed by rates of vertical uplift or subsidence, has varied sharply along the coast of Kamchatsky Peninsula during the past ~2000 yr (Table 2; Fig. 6). Averaged over the longest time interval (A.D. 250–2000), the fastest uplift has been on the western side of Kamchatsky Cape (up to 6.8 mm/yr) and on Cape Africa (up to 6.6 mm/yr). On other parts of the coast, the average uplift rates have been lower (ranging from 0.5 to 4.6 mm/yr), and some parts of the coast have experienced net subsidence or stability.

Based on our data and analysis, we divide the south and central eastern coast of the peninsula into four parts (Fig. 6), which differ by rate of vertical deformation, from south to north:

(1) Kamchatsky Cape has a high uplift rate, with the highest rate at profile 23, the last preserved Holocene terrace in our traverse toward the west;

(2) The coast between profiles 10 and 19, including the Pikezh and First Pereval'naya River valleys, shows prevalent net stability or subsidence for the past 2000 yr. All progradational terraces along this part of the coast (which easily can be seen in the Google Earth images) are very young and typically do not contain any tephras or just the tephra from A.D. 1964. We assume that net subsidence during earthquakes could explain the lack of the older terraces here, despite the large sediment supply and high recent accumulation rate.

(3) Cape Africa and neighboring coastal areas have a high uplift rate.

(4) The coast north of Second Pereval'naya River to Soldatskaya Bay has low to moderate rates of net uplift. For this zone, we have limited data from Holocene terraces, but well-preserved Pleistocene terraces (Pedoja et al., 2006, 2011) improve our conclusion about the general direction of vertical movement.

Uplift on Capes Africa and Kamchatsky took place during all analyzed time intervals. For other parts of the coast, the direction of vertical deformation was time variant, that is, there are profiles where no terrace contains a particular marker tephra in the basal position; in these cases, we interpret that record to have been eroded during a period of subsidence (Fig. 6). Preserved (uplifted) erosional scarps on profiles (e.g., Fig. 4) are also suggestive of episodes of subsidence, even if tephras remain preserved, because sharp and high scarps are not present on prograding coastlines (e.g., lower parts of profiles 8 and 22 in Fig. 2).

Periods of coastal erosion could be associated with two main factors—relative sea-level rise and changes in sediment supply. We think

TABLE 2. VERTICAL DEFORMATION RATES CALCULATED FROM HOLOCENE COASTAL TERRACES

			1750 B.P.–0 B.P.		1400 B.P.–0 B.P.		1400 B.P.–1750 B.P.	
Profile (N to S)	Profile latitude* (°N)	Profile longitude* (°E)	Vertical offset rate (mm/yr)	Net error (±mm/yr)	Vertical offset rate (mm/yr)	Net error (±mm/yr)	Vertical offset rate (mm/yr)	Net error (±mm/yr)
New (a)	56.45338	163.24941	1.04	0.05	1.22	0.04	0.34	0.13
Northern (b)	56.45177	163.24921	2.21	0.14	2.30	0.12	1.86	1.01
Southern (c)	56.44438	163.24833	1.70	0.11	1.48	0.08	2.6	1.41
Camp (d)	56.43522	163.25758	1.25	0.08	0.99	0.05	2.29	1.24
Black Rock N (e)	56.41825	163.28912	0.53	0.03	†	†	†	†
Black Rock S (f)	56.41127	163.29349	2.32	0.15	1.52	0.08	5.54	3.01
Cape Reef (h)	56.32710	163.35305	†	†	2.02	0.11	†	†
3/4	56.25153	163.33766	~4.6§	†	†	†	†	†
2	56.24913	163.33786	~4.0§	†	†	†	†	†
1	56.24860	163.33796	†	†	2.5§	0.3	†	†
5	56.23052	163.34330	1.83	0.12	†	†	†	†
6	56.22231	163.34555	6.38	0.41	6.45	0.34	6.09	3.30
7	56.21445	163.34630	6.15	0.40	4.52	0.24	12.78	6.94
181	56.20509	163.34962	5.12	0.33	4.89	0.26	6.06	3.29
8	56.19693	163.35201	6.49	0.42	3.41	0.18	19.03	10.33
9	56.18995	163.35911	6.55	0.42	4.91	0.26	13.23	7.18
14	56.18071	163.34413	†	†	4.44	0.23	†	†
13	56.17326	163.32295	†	†	3.62	0.19	†	†
11	56.16215	163.29628	4.20	0.27	3.91	0.21	5.37	2.92
10	56.15418	163.28801	4.53	0.29	†	†	†	†
16	56.13075	163.17356	–1.04	0.07	†	†	†	†
18	56.09948	163.12281	~1.8§	†	†	†	†	†
19	56.09386	163.11398	~3.7§	†	†	†	†	†
20	56.03191	163.05925	1.64	0.11	1.75	0.09	1.17	0.64
21	56.02541	163.05508	2.84	0.18	2.62	0.14	3.72	2.02
22	56.01826	163.04913	3.43	0.22	3.47	0.18	3.29	1.78
23	56.01828	162.96598	6.79	1.61	4.89	0.26	8.77	4.71

*In most cases, longitude and latitude are at the shoreline; in others, excavation closest to shoreline.
†Record is eroded; cannot calculate offset or error.
§Calculated from river level near mouth.

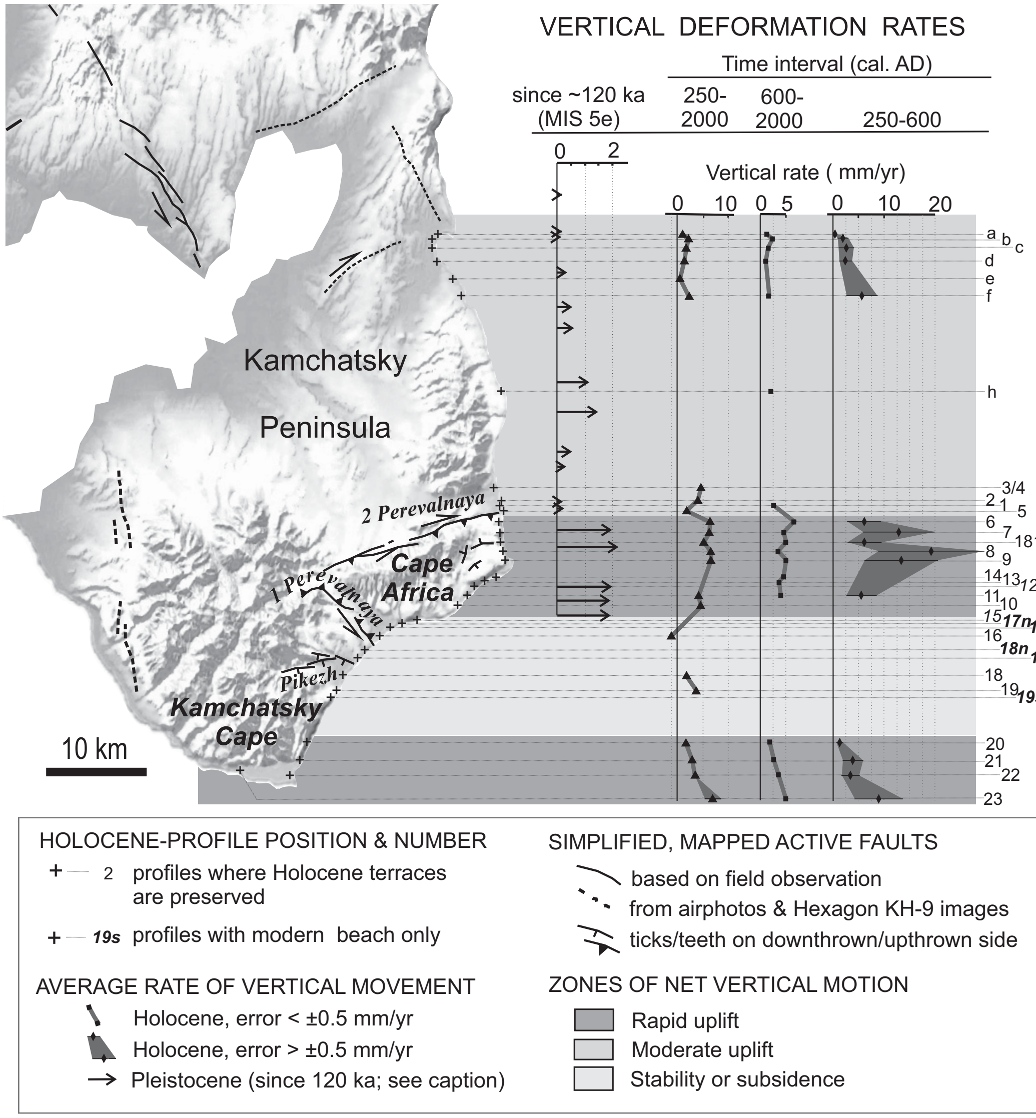

Figure 6. Summary of calculated and inferred rates of vertical deformation along the open coast of the Kamchatsky Peninsula for the late Holocene (past ~2000 yr; this paper) and for the latest Pleistocene (past 120,000 yr, since marine oxygen isotope stage [MIS] 5e; Pedoja et al., 2006). The methods for calculating Holocene rates are discussed in detail in this paper (see also Fig. 5; Table 2; DR2 [see text footnote 1]). Mapped active faults are based on Kozhurin (2007, 2012) and Kozhurin and Pinegina (2011).

that on the Kamchatsky Peninsula, on a millennial time scale over the late Holocene, terrace erosion is mostly indicative of (tectonic) coastal subsidence, which in effect is a local sea-level rise, leading to beach-scarp development and landward retreat (as in Meyers et al., 1996; Saltonstall and Carver, 2002). Our reasoning for this conclusion is based on an assumption that there were no big changes in sediment supply and wave energy during the past ~2000 yr. This coastline does not have an accumulative estuarine (coastal marsh) setting such as has been used on a number of coastlines to examine periods and episodes of subsidence (e.g., Atwater and Hemphill-Haley, 1997; Shennan et al., 1998). It possible to calculate a rate of subsidence only for one of the profiles (profile 16), where the subsided part of the terrace including tephra is partially preserved in a coastal alluvial plain. However, almost all the uplifted profiles have preserved steep scarps and sharply truncated tephra in excavations, suggesting episodes of erosion (we think due to subsidence), and then uplift to preserve the scarp in relief (e.g., Fig. 4; Figs. DR1–DR2 [see footnote 1]).

For profiles 15, 17n, 17s, 18n, 18s, and 19s (position of profiles shown on Fig. 6), it was not possible to calculate rates of vertical deformation for any of the chosen time intervals. On these profiles, young Holocene terraces (younger than ca. A.D. 600) directly adjoin Pleistocene sequences, with no older Holocene terrace presence.

Data on profiles 1, 2, 3/4, 18, and 19 may yield a slightly higher rate of vertical deformation than in reality because they were measured not from the dv point but from the river level near the river mouth. The river level near the river mouth is approximately the same as sea level or slightly higher and could vary in time due to river mouth migration.

The highest uplift rates and the highest gradients of rate change along the coast are recorded during the shortest time interval (~350 yr, assigned age bracket A.D. 250–600; Fig. 6). For example, during this short time interval, the coast along Cape Africa (profiles 7, 181, 8, 9) experienced an uplift rate of up to 19 mm/yr. This fact supports our interpretation that major strain-releasing seismicity best explains the history of vertical coastal deformation. A few coastal localities (e.g., profiles 18, 19) that experienced net slow uplift during the past 2000 yr apparently experienced net subsidence after the time of SH_{1450} (A.D. 600) ash fall, because this ash is not preserved in terraces closer to the shoreline than those also containing KS_1 (A.D. 250).

Despite the relatively fast late Holocene (last 2 ka) uplift rates around Capes Africa and Kamchatsky, there is almost no preservation of relic (soil-blanketed) marine terraces formed between ca. 2 ka and ca. 5 ka (ca. 5 ka taken to be the end of the mid-Holocene highstand; Woodroffe and Horton, 2005). Given that regional postglacial sea levels stabilized in the mid-Holocene, and given the more recent net uplift rates, we would expect these older, uplifted Holocene terraces to be preserved, as they are on other Kamchatka coastlines, even those that do not experience much uplift (Pinegina et al., 2002, 2003, 2012; Bourgeois et al., 2006). Thus, on southeast Kamchatsky Peninsula, we can interpret the absence of terraces between ca. 2 ka and ca. 5 ka to represent (1) a period of net subsidence, or (2) a period of stability on a background of low sediment supply and coastal erosion. We favor a neotectonic explanation such as coseismic (or interseismic) subsidence because the erosional period appears to be more or less synchronous from Kamchatsky Cape to south of Soldatskaya Bay, but it does not include other coastal areas of net stability or subsidence (Soldatskaya, Stolbovaya, Ust'Kamchatsk regions, Fig. 2). In areas of most rapid uplift, such as Cape Africa (and perhaps buried under alluvial fans at Kamchatsky Cape), fragments of these terraces are preserved (Fig. DR1 [see footnote 1]).

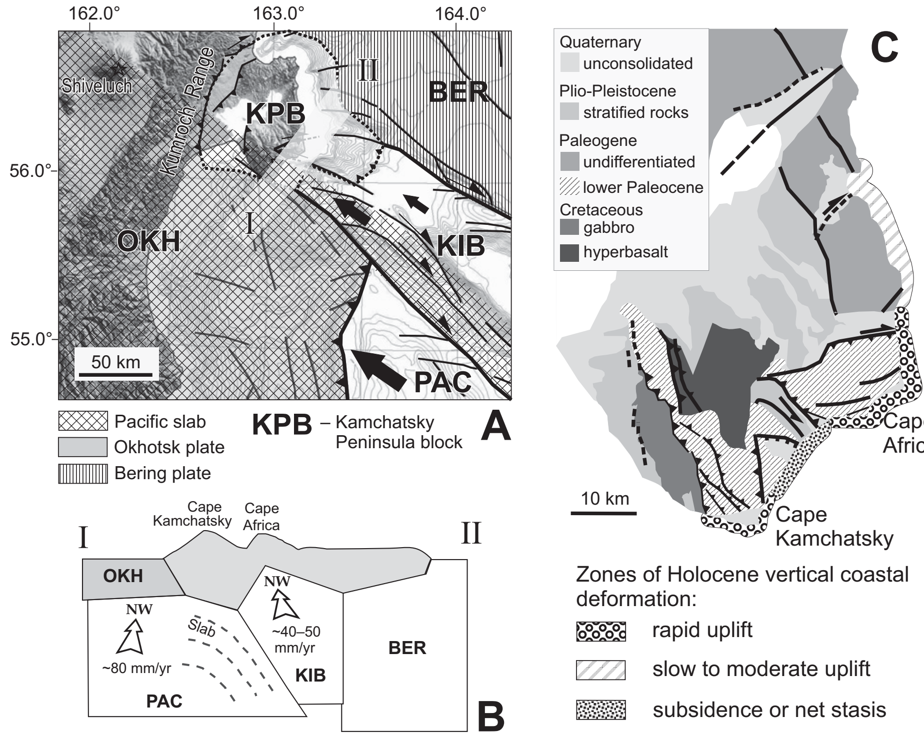

Figure 7. Proposed geodynamic model for the Kamchatsky Peninsula region. (A) Proposed boundary of Kamchatsky Peninsula block (KPB): Western onshore boundary is after Kozhurin (2009) and Kozhurin and Pinegina (2011); other boundaries are shown schematically; southern boundary is after Bourgeois et al. (2006) and Pedoja et al. (2006); northern and eastern boundaries are shown along the base of the continental slope (margin). I-II—position of the schematic cross section shown on B. (B) Schematic cross section of the Kamchatsky Peninsula region divided into plates. PAC—Pacific plate, BER—Bering plate, OKH—Okhotsk plate, KIB— Komandorsky [Commander] Island block. Okhotsk and Pacific plates extend to the northwest, Komandorsky Island and Bering plates are limited by the Kamchatsky Peninsula block. (C) Geological map of Kamchatsky Peninsula (modified from Freitag et al., 2001), showing its main structural features and main faults, both active and old and zones of Holocene vertical coastal deformation. Note that the faults in C are based on different interpretations than in A.

DISCUSSION

Sources and Types of Deformation

Along the coastal zone encompassing Kamchatsky Peninsula, thrust, oblique strike-slip, and normal crustal faults occur onshore and offshore; thus, we expect complex patterns of coastal deformation at individual sites (represented by profiles and groups of profiles). Below the surface, the Pacific plate is subducting south of and terminating near the Kamchatsky Peninsula (Figs. 1 and 7). The Komandorsky Island block and the Bering plate are impinging on the central and northern Kamchatsky Peninsula. At its western boundary, the Kamchatsky Peninsula block collides with the Okhotsk plate (or North America plate); this recent interaction is supported by the existence of active thrust and strike-slip faults along the eastern boundary of the Kumroch Range (Kozhurin, 2009; Kozhurin and Pinegina, 2011; Fig. 7A).

Differentiated vertical deformation of the Kamchatsky Peninsula coast can be interpreted as a net result of coseismic and interseismic movement. Support for this interpretation comes from the pattern of the historical leveling record (Fig. 3) spanning two different kinds of earthquakes (1971 and 1984) and an interseismic period, which mimics the longer-term records (Fig. 6). At least a part of individual abrupt vertical deformation can be caused by elastic coseismic coastal deformation, such as occurred in 1971 and 1984, and as has been shown for many coastlines (Barrientos and Ward, 1990; Carver et al., 1994; Merritts, 1996; Briggs et al., 2008). However, brittle faulting is also responsible for some of the change, as is apparent in the sharp changes in uplift rates across onshore active crustal faults, such as along the Second Pereval'naya River. In other words, some of the deformation comes from offshore faults that may not directly underlie the peninsula, and some of the deformation comes from faults that are on the peninsula, in the area surveyed. The length (only kilometers to tens of kilometers) of onshore faults on Kamchatsky Peninsula may preclude very large events. However, we cannot rule out the possibility of deformation associated with a large rupture of the northern end of the Kamchatka subduction zone or along the Pacific-Aleutian boundary (Fig. DR4 [see footnote 1]).

Rates and Directions of Deformation versus Length of Observed Time

On the Kamchatsky Peninsula, Holocene vertical deformation shows similar patterns to historical and Quaternary records, with the shortest-interval Holocene rate (A.D. 250–600) comparable to the historical leveling data and up to ten times faster than the latest Pleistocene–derived rate (Fig. 6). We think that the short-term Holocene record tends to reflect a few individual events, with little time averaging. The Kamchatsky Peninsula historical data include two earthquakes of different origins, both producing the same sense of uplift and subsidence where recorded (Figs. 1 and 3), and a net scale of deformation comparable to the short-term Holocene rate (A.D. 250–600). However, with the tectonic setting of the Kamchatsky Peninsula, it is not appropriate to interpret this time span as a seismic cycle because there are several potential sources of deformation events, each involving a different sense and amount of deformation.

The intermediate-interval rates (for the past ~2000 yr) are 2–3 times faster than Pleistocene rates (Fig. 6; Fig. DR5 [see footnote 1]). Such differences in tectonic-movement rates averaged for time intervals that differ in duration, and the increase of these rates toward the present, have been established for many coasts of tectonically active regions of the world (Lajoie, 1986, his Fig. 6.11; Ota and Yamaguchi, 2004) and have been discussed in general by Gardner et al. (1987) (Fig. DR5 [see footnote 1]). However, there are areas where the rates do not appear to change as much (e.g., McSaveney et al., 2006).

Looking at the period with the highest rate of uplift (A.D. 250–600), we see evidence for multiple earthquake events (terraces and scarps), as discussed in the following, although all events may not be recorded in the coastal stratigraphy. It is likely that large earthquakes, which generated greater coastal deformation than the 1971 or 1984 earthquakes, played a role in this uplift. Concerning the probability of several events, we took into account that even if not all vertical coseismic deformation was preserved (due to interseismic recovery), the net uplift of Cape Africa during ~350 yr was 6.5 m and that of Kamchatsky Cape was up to ~3 m. We think it is more likely that such large amounts of uplift are the sums of two or three events rather than one. The time interval of 350 yr is long enough to include several large seismic events, and profiles typically show two to three geomorphic features (beach ridges at different elevations, sometimes separated by erosional scarps) between the last occurrence of KS_1 and the last occurrence of SH_{1450} (e.g., Fig. DR1 [see footnote 1]).

The intermediate-interval Holocene vertical rates (A.D. 250–2000, A.D. 600–2000) are still 2–3 times higher than latest Pleistocene rates (Fig. 6), but they begin to average out the noise of individual events. The fact that in a few cases (see Table 2; Fig. 6) the rates for A.D. 250–2000 show higher net uplift rates than those for A.D. 600–2000 indicates that episodes of subsidence occurred that caused the latter rate to be lower (or episodes of uplift that caused the former rate to be higher). A steep scarp just seaward of the last incidence of SH_{1450} supports the subsidence hypothesis (Fig. 4; Fig. DR2 [see footnote 1]). However, even with evidence for subsidence in this interval, uplift rates exceed Pleistocene rates by a significant amount. Another possibility is that the long-term net rates have increased from Pleistocene to Holocene, but we do not have a reason to support this assumption because the regional tectonic/geodynamic regime typically does not change significantly over on this time scale.

For most of the Kamchatsky Peninsula coastline, we cannot determine a deformation rate for the past 4000–5000 yr because the record from ca. 2 to 5 ka (and older) has been eroded. The loss of this record may to indicate that regions of net uplift in the past 2000 yr may have been characterized by net subsidence in the prior few millennia in the southeast Kamchatsky Peninsula. In contrast, other coastal sites on Kamchatka preserve wave-built terraces older than ca. A.D. 250 (up to 3000 B.C. or mid-Holocene; Bourgeois et al., 2006; Pinegina et al., 2002, 2003, 2012).

One potential test of the significance of time-interval differences in uplift rates is to compare them with the paleotsunami record for the late Holocene of the Kamchatsky Peninsula (Fig. DR6; see footnote 1]); this record is a proxy for large earthquakes such as in 1971 (Martin et al., 2008). Because most tsunamis are coseismic, our analysis would predict that there would also be more frequent tsunamis recorded in shorter time intervals, and that over the long term, there may be more- and less-active periods of tsunami recurrence. At nearby localities to the north (Stolbovaya and Ozernoi; Figs. DR6a and DR6b [see footnote 1]), this prediction appears to hold, with the notable exception of the KS_1–SH_{1450} interval, where there is an inverse relationship of time interval between tephras with recurrence rate of tsunami deposits therein.

Along the 34 profiles measured for this study of Kamchatsky Peninsula, there appears to be a positive correlation of vertical deformation rate (Fig. 6) and tsunami recurrence rate (Figs. DR6c and DR6d [see footnote 1]). At Soldatskaya Bay, there are up to three tsunami deposits between tephra KS_1 (A.D. 250) and SH_{1450} (A.D. 600), which is a higher recurrence rate than above or below that interval (Fig. DR6c [see footnote 1]). Along the Kamchatsky coast (Fig. DR6d [see footnote 1]), there are up to five tsunami deposits between these two tephras (2–4 being common). On the longer term, at Soldatskaya Bay, in the period ca. 1500 B.C. to A.D. 250, the recurrence of tsunami deposits is lower than for ca. A.D. 250 to A.D. 2000 or for 2000 B.C. and 1500 B.C. (base of record). This trend of fewer tsunami deposits in ca. 2000 B.C. to A.D. 250 than A.D. 250 to A.D. 2000 is repeated at other sites along the east coast of Kamchatka (e.g., Pinegina et al., 2003). Most of Kamchatsky Peninsula has a shorter record, but the fewer tsunami deposits at other sites (Figs. DR6a and DR6b [see footnote 1]; Pinegina et al., 2003) correlate with the few to no preserved terraces on southeast Kamchatsky Peninsula during the period which we interpret to be a time of net stasis or subsidence and erosion.

Correlation of Terrace Deformation Patterns with Active Faults of Kamchatsky Peninsula

We compared measured differences in coastal vertical deformation with active faults onshore of the Kamchatsky Peninsula that intersect the shoreline (Kozhurin 1985, 1990, 2004, 2007, 2012; Gaedicke et al., 2000; Freitag et al., 2001; Baranov et al., 2010; Kozhurin and Pinegina, 2011) to determine if some deformation events may have occurred on these faults. The concordance of active faults with distinct changes in Holocene uplift rates is distinct (Figs. 6 and 7; also see Fig. 1), and thus we conclude that some coseismic-deformation events in the past 2000 yr have occurred on these mapped faults. Of course, offshore faults could also be responsible for coseismic deformation, as illustrated, for example, on the North Island of New Zealand (Berryman et al., 2011) and as modeled for the Taiwan coast (Huang et al., 2010). Some vertical deformation could be as folding due to blind faults.

Second Pereval'naya River Valley

An active fault has been mapped, trending west-southwest from the mouth of the Second Pereval'naya River upstream to the drainage of the First Pereval'naya River (Fig. 6). There is general agreement that this fault exhibits right-lateral slip with a thrust component (south side up; e.g., Gaedicke et al., 2000; Freitag et al., 2001), with Freitag et al. (2001) suggesting that this fault is the onshore extension of a branch of the Bering transform zone (Fig. 1). From cumulative slip measured in trenches across the fault and from offset of geomorphic features, rates of lateral offset for the Holocene range from ~4.5 mm/yr in the western part (Kozhurin, 2007) to ~15–20 mm/yr in the eastern part (Kozhurin, 2012). The same techniques have yielded relative vertical components up to 7–8 mm/yr near the coast (Kozhurin and Pinegina, 2011).

This fault (or splay of a fault zone) at the coastline is situated between our profiles 5 and 6 (N to S). The uplift difference calculated from Holocene terraces on profiles 1 and 5 north of the fault and profile 6 south of the fault is ~3–5 mm/yr (Fig. 6; Table 2), and we would agree that this offset is taken up along the fault zone. Based on the different elevation of the older (Pleistocene) marine terraces across this fault, this change in uplift rate is persistent (Fig. 6). We conclude that the fault zone along the Second Pereval'naya River coincides very well with the southern boundary of the moderately uplifting Cape Reef block and the northern boundary of a rapidly uplifting Cape Africa block (Figs. 6 and 7). Because the Second Pereval'naya River fault deforms the present shoreline, we assume that this fault continues (some distance) offshore. However, there is no evidence for a connection with the Bering transform zone.

First Pereval'naya River Valley

On the geological map of Kamchatsky Peninsula (Markovskiy et al., 1989; Boyarinova et al., 1999; see also Freitag et al., 2001), there is a mapped or suggested onshore fault on the north side of the First Pereval'naya River valley (Fig. 7), although this fault is not mapped in Baranov et al. (2010). This fault would lie to the south of our profile 10, where there is a distinct change in the pattern of Holocene terraces (Fig. 6). At profile 10, there is a net uplift rate of ~4.5 mm/yr since A.D. 250, whereas to the south, the nearest profile for which we have data (16) has a net subsidence rate of –1 mm/yr. Thus, our data suggest that south of profile 10, there is a fault, which is north side up, and the pattern of deformation suggests it is a thrust fault bounding the southern side of Cape Africa. This fault extends from land at least to the shoreline, but we do not have specific evidence to tie it to an offshore structure. Baranov et al. (2010, and earlier papers) extended the Pikezh transform zone into the First Pereval'naya River valley (with two or more strands), whereas Kozhurin (2007) "stopped" this transform zone at the shelf edge. Geophysical mapping on the continental shelf is needed to resolve this problem.

A NW-striking fault has been mapped on the south side of the First Pereval'naya River valley (Fig. 6), but we cannot see the fault in Holocene marine terraces (Fig. 6), likely because this portion of the coast is eroded and has only young Holocene sediment (not older than 100–200 yr). Kozhurin (1985) interpreted this fault as predominantly normal, Gaedicke et al. (2000) and Freitag et al. (2001) as right lateral with some thrust component, and Baranov et al. (2010) as predominantly left lateral. From more recent field data, Kozhurin (2012) made three trenches across this fault and reinterpreted it as predominantly thrust (north side up) with a small left-lateral component. This fault intersects the coast between profiles 16 and 18n (N to S).

Pikezh River Valley

The coast between the First Pereval'naya and Pikezh Rivers is currently aggrading (based on our field data and satellite images). The existence here of only a very young marine terrace (with only one preserved tephra, Sh_{1964}) indicates earlier Holocene subsidence. Older fluvial terraces are present along both rivers, but Pleistocene marine terraces are not evident. We interpret this region to be one of net stasis or subsidence.

The Pikezh River valley lies within this area of Holocene net subsidence, based on the preservation of only young terraces (Fig. 6). The Pikezh valley near the river mouth is very wide and box-like due large-amplitude horizontal river migration. In our interpretation, this migration is a result of sediment accumulation and net subsidence. The large volume of sediment in the Pikezh River is transported from a zone of highly deformed sedimentary rock (Markovskiy et al., 1989; Boyarinova et al., 1999). The preserved Holocene fluvial terraces at the Pikezh River mouth are young, not older than 2000 yr B.P., also providing evidence of net Holocene subsidence of this zone.

Kozhurin (2007) mapped a normal fault on the north side of Pikezh valley, south side down; this fault as mapped emerges at the shore between our Holocene profiles 18s and 18. From our data, we do not see the exact point on the coast where this fault affects Holocene terraces because there are not young terraces in this stretch of coastline. The location of this normal fault fits well with net coastal subsidence in this area. Both the First Pereval'naya and Pikezh valleys lie within the predominantly subsiding stretch of the coast that separates the uplifting Capes Kamchatsky and Africa from each other (between our profiles 15 and 20). These drainages were identified by Freitag et al. (2001) as a region with higher exhumation rates than Cape Africa since the Pliocene (their Fig. 9). Exhumation certainly fits with the high progradation rate at the coast, but in our interpretation, it does not indicate a high uplift rate but rather the high rate of erosion of altered sedimentary rock upstream. The existence of landslides at the upper part of Pikezh River supports this conclusion.

Kamchatsky Cape Region

While modern topography rises south of the Pikezh Valley, there are no ca. 2000 and ca. 1500 yr B.P. Holocene terraces preserved between the valley and profile 20 (Fig. 6). The three Holocene profiles on the east side of the cape show mild tilting up to the south, which would be consistent with subsidence north of profile 20. Profile 23 is in a different deformation regime on the west side of Kamchatsky Cape and shows a high rate of uplift. No recent studies (Freitag et al., 2001; Kozhurin, 2004, 2007; Baranov et al., 2010) show active faults on the coast near Kamchatsky Cape that would account for this change in deformation rate. On the massif north of Kamchatsky Cape, Baranov et al. (2010) showed some small, active normal faults on maps.

Geodynamics as Reflected in Marine Terraces

Kamchatsky Peninsula is situated in a very complex geodynamic setting, which is why the character of deformation is ambiguous and hard to model.

The analysis of existing seismological and geodetic data (Fedotov et al., 1985; Gordeev et al., 2006; Levin et al., 2002, 2006; Levin, 2009; Mackey et al., 2010) shows that Kamchatsky Peninsula itself is situated in conditions of prevalent compression oriented NW-SE; directly offshore (to the east), the dominant mode of deformation is strike slip. Vertical displacements as expressed in the marine terraces are differentiated in space and in time by rate and in some cases by direction (Fig. 6). A distinctive aspect of the pattern of deformation along the outer Kamchatsky Peninsula is its variability over relatively short distances, with some zones "popping up" quite rapidly, while others are stable, subsiding, or slowly uplifting (Fig. 7).

Seismicity, GPS records, and geomorphic and geologic analysis of active faulting and marine terraces suggest that the shallow part of the Kamchatsky Peninsula is being "bulldozed" from the east and less so from the south and north by the Komandorsky Island block and the Okhotsk and Bering plates, as well as the subducting Pacific plate (Fig. 7; Fig. DR4 [see footnote 1]). The active uplift on the outer edges of the peninsula is the effect of this collision with the surrounding plates. Geomorphologically, the peninsula looks like a (half) bowl with a low interior and steep edges. Differential movement along the coast of the peninsula is partially the result of the interaction with different plates, leading to the heterogeneity of coastal tectonic behavior.

On a smaller scale, the presence and behavior of Cape Africa may also be related to indentation. Cape Africa as a block is moving in the same general sense as offshore transform zones (e.g., Baranov et al., 2010), with a late Holocene horizontal rate of ~15–20 mm/yr (Kozhurin, 2012) and vertical coastal uplift rate of ~5–7 mm/yr (this study). We disagree with Baranov et al. (2010) that the GPS-measured inland motion at Krutoberegovo can be directly assigned to Cape Africa; the difference in rate of 35–50 mm/yr horizontal motion for Komandorsky Island and 8–15 mm/yr for Krutoberegovo must be taken up somehow between the two, and there is no evidence that the rest of the Kamchatsky Peninsula and Cape Africa are acting as a rigid block. Our data show that it is more likely not rigid. The difference in GPS speed for the Komandorsky Island block and Krutoberegovo area may also reflect incomplete coupling of the peninsula with the underthrusting plate, which below Kamchatsky Peninsula may or may not have an older chunk of thicker Komandorsky crust in contact with Kamchatka crust. The thrust belt of the Kumroch Range implies that some westward block motion is taken up by this crustal deformation.

Our data from Kamchatsky Cape indicate moderate to rapid uplift rates, with a faster rate on the (south)western side. We do not have enough data to say that Cape Kamchatsky is one block; it may be divided by a series of faults on a number of smaller blocks. The southern boundary of the Kamchatsky Peninsula (if it is not a part of the Okhotsk plate) corresponds to the "edge" of the Okhotsk plate and a projected Pacific plate below (Fig. 7). We think that Kamchatsky Cape and indeed the entire southern part of the Kamchatsky Peninsula, driven primarily by the movement of the Komandorsky Island block, may have an oblique thrust boundary with the Okhotsk plate (Fig. 7).

The interaction of Kamchatsky Peninsula with the Pacific plate is distinctly different from its interaction with the Bering and Okhotsk plates and Komandorsky Island block because there is no surface expression of the boundary. The effect of the Pacific plate is apparent along the northern edge of the Pacific slab, where earthquakes off the Kamchatsky Strait bend northwest of the subduction zone, and to the northeast under the Kamchatsky Peninsula to a depth of ~100 km (Pinegina et al., 2010). Interaction with the subducting slab can lead to the appearance of southwestern tangential stress on the base of southern Kamchatsky Peninsula (Fig. 7). The possibility of tangential stress from the Pacific slab can explain the existence of unusual (for a "squeezing peninsula" tectonic model) normal faults along the Pikezh River.

There is no simple explanation for *net* subsidence of all southeastern Kamchatsky Peninsula during the time interval from roughly 2000 to 5000 yr B.P. (note that uplift events could have occurred during this time, as well). One possibility is a giant subduction zone earthquake that has an average recurrence interval longer than 2000 yr. In this regard, we draw attention to the similarity of the overall structure of the western Aleutian arc (including the Kamchatka Peninsula) and the Sumatra-Andaman region (Geist et al., 2006; Lander and Pinegina, 2010). In both cases, an oceanic plate submerged under the island arc moves rapidly along the strike of the arc, carrying along transform fault slivers (split-off segments of the arc). This may suggest the possibility of an earthquake similar to the Sumatra-Andaman event in 2004 at the west end of the Aleutian arc (Fig. DR3 [see footnote 1]). Geist et al. (2006) also listed the Komandorsky sector of the Aleutian subduction zone as potentially dangerous and capable of launching a major tsunami southward. Many but not all subduction-zone earthquakes show this behavior.

On the other hand, a great earthquake could also occur in the northern part of the Kamchatka subduction zone (Fig. DR3 [see footnote 1]). However, we do not know if one (or a few) exceptionally large events could have caused so much subsidence that almost all of the 2000–5000 yr B.P. depositional sequence of coastal Kamchatsky Peninsula south of Soldatskaya Bay was erased. Our observations just south of Ust'-Kamchatsk (Fig. 2) support the possibility of a great earthquake in the northern part of the Kamchatka subduction zone because all Holocene beach ridges older than ca. 3000 B.P. have also been erased there (Pinegina et al., 2012).

Great subduction earthquakes accompanied by coastal subsidence could explain why the average uplift rates of the Pleistocene terraces (120 ka and older; Pedoja et al., 2006; Fig. 6) are two to three times less than rates obtained using Holocene terraces from the past 2000 yr, in the same coastal zones. Not enough time has passed for the Holocene record to average out events with such long recurrence intervals.

CONCLUSIONS

Vertical deformation of the southeast Kamchatsky Peninsula averaged over the past ~2000 yr ranges from approximately –1 to +7 mm/yr. The most intensive and continuous Holocene vertical uplift has taken place around Capes Africa and Kamchatsky, consistent with their being uplifted mountainous massifs generated over a longer time scale. Sharp changes in rate of uplift in the Holocene correspond to three known active faults along the Pikezh, First, and Second Pereval'naya Rivers.

In individual locations, the average rate of vertical deformation varies over different time intervals and even changes from net uplift to subsidence. Through comparison of our data with seismological and geodetic data, we hypothesize that deformation of marine terraces was most likely coseismic. Earthquake source locations might be on mapped onshore and offshore faults as well as on unmapped faults under the continental shelf. Some coseismic deformation could be realized during the slip of the Pacific slab at its NW corner. The highest gradients of rate change along the coast took place during the shortest time interval we analyzed (~350 yr long). This supports our conclusion that it is coseismic deformation rather than slow tectonic movement. There is some suggestion that the net rates for the past 2000 yr include episodes of both uplift (raised terraces) and subsidence (completely or partly eroded terraces).

We see no reason to assign the same rate of lateral displacement to the Cape Africa block as to Krutoberegovo station (as in Baranov et al., 2010); also, it seems clear that the Cape Africa block is not moving at the same rate as the Komandorsky Island block. If the GPS measurements represent a longer-term trend (such as the Holocene or longer), then the shortening could be taken up either offshore (suggested by Baranov et al., 2010) or onshore or, most likely, both. The dramatic difference in uplift between Cape Africa and the subsiding area to the south suggests to us that there should be a thrust fault bounding the southern side of the cape.

We propose a qualitative explanation for the variety of vertical movements observed on the Kamchatsky Peninsula coastline. The shallow parts of the Kamchatsky Peninsula are pressed (squeezed) between three bounding plates—Bering, Okhotsk, and Komandorsky Island block—whereas the base is partly coupled with the Pacific slab (Fig. 7). We think that in the northern and northeastern part of the peninsula, deformation is primarily the result of interaction with the Bering plate, resulting in slow to moderate uplift. Cape Africa rises rapidly as a result of collision with the Komandorsky Island block. The southern and western parts of the peninsula are under the influence of two plates: interaction with the Okhotsk plate and tangential stress on the base as result of coupling with the Pacific slab. This geodynamic model helps explain the pattern of coastal uplift and subsidence described in detail in this paper.

ACKNOWLEDGMENTS

Our co-author and dear friend Katya Kravchunovskaya died in winter 2013 during a mountaineering rescue on Avachinsky volcano; we miss her terribly. This research has been supported primarily by grants from the Russian Foundation for Basic Research (03-05-64584 to Pinegina) and the U.S. National Science Foundation (EAR-9903341 and EAR-0125787 to Bourgeois). Collaborative writing was facilitated by hosted visits to the Institute of Volcanology and Seismology FEB RAS (JB), Hokkaido University Institute of Seismology and Volcanology (TP, JB), and the University of Caen (JB). Field assistance was provided in particular by Alexander Storcheus, Roman Spitsa, Ivan Storcheus, Mstislav Sokolovsky, and Victor Morozov. SeanPaul LaSelle shared his profiles of Dembi Spit, east of Ust'Kamchatsk. Special thanks go to Vera Ponomareva for discussion and review of tephra stratigraphy and to Andrey Kozhurin for discussions about active faults and geodynamics. We thank reviewers Ursula Cochran, Maury McSaveny, Alan Nelson, and Dave Scholl for their thoughtful comments and suggestions.

REFERENCES CITED

Alexeiev, D.V., Gaedicke, C., Tsukanov, N., and Freitag, R., 2006, Collision of the Kronotskiy arc at the NE Eurasia margin and structural evolution of the Kamchatka–Aleutian junction: International Journal of Earth Sciences, v. 95, p. 977–993, doi:10.1007/s00531-006-0080-z.

Apel, E.V., Bürgmann, R., Steblov, G., Vasilenko, N., King, R., and Prytkov, A., 2006, Independent active microplate tectonics of northeast Asia from GPS velocities and block modeling: Geophysical Research Letters, v. 33, L11303, doi:10.1029/2006GL026077.

Atwater, B.F., and Hemphill-Haley, E., 1997, Recurrence Intervals for Great Earthquakes of the Past 3,500 Years at Northeastern Willapa Bay, Washington: U.S. Geological Survey Professional Paper 1576, 108 p.

Baranov B., Gaedicke C., Freitag R., and Dozorova, K., 2010, Active faults of south-eastern Kamchatsky Peninsula and Komandorsky shear zone: Vestnik KRAUNTS Nauki o zemle, v. 16, p. 66–77 (in Russian).[2]

Barrientos, S., and Ward, S., 1990, The 1960 Chile earthquake: Coseismic slip from surface deformation: Geophysical Journal International, v. 103, p. 589–598, doi:10.1111/j.1365-246X.1990.tb05673.x.

Berryman, K., Ota, Y., Miyauchi, T., Hull, A., Clark, K., Ishibashi, K., Iso, N., and Litchfield, N., 2011, Holocene paleoseismic history of upper-plate faults in the southern Hikurangi subduction margin, New Zealand, deduced from marine terrace records: Bulletin of the Seismological Society of America, v. 101, p. 2064–2087, doi:10.1785/0120100282.

Bookhagen, B., Echtler, H.P., Melnick, D., Strecker, M.R., and Spencer, J.Q.G., 2006, Using uplifted Holocene beach berms for paleoseismic analysis on the Santa María Island, south-central Chile: Geophysical Research Letters, v. 33, L15302, doi:10.1029/2006GL026734.

Bourgeois, J., Pinegina, T.K., Ponomareva, V.V., and Zaretskaia, N.E., 2006, Holocene tsunamis in the southwestern Bering Sea, Russian Far East, and their tectonic implications: Geological Society of America Bulletin, v. 118, p. 449–463, doi:10.1130/B25726.1.

Boyarinova, M.E., Vishnyakov, N.A., Korkin, A.G., Saveliev, D.P., and Markovskiy, B.A., eds., 1999, State Geological Map of the Russian Federation: East Kamchatka Series Sheets O-58-XXVI, XXXI, XXXII: Saint-Petersburg, VSEGEI (A.P. Karpinsky Russian Geological Research Institute), scale 1:200,000 (in Russian with English legend).

Braitseva, O.A., Ponomareva, V.V., Sulerzhitsky, L.D., Melekestsev, I.V., and Bailey, J., 1997, Holocene key-marker tephra layers in Kamchatka, Russia: Quaternary Research, v. 47, p. 125–139, doi:10.1006/qres.1996.1876.

Briggs, R.W., Sieh, K., Amidon, W.H., Galetzka, J., Prayudi, D., Suprihanto, I., Sastra, N., Suwargadi, B., Natawidjaja, D., and Farr, T.G., 2008, Persistent elastic behavior above a megathrust rupture patch: Nias island, West Sumatra: Journal of Geophysical Research, v. 113, B12406, doi:10.1029/2008JB005684.

Burbank, D.W., and Anderson, R.S., 2001, Tectonic Geomorphology: Oxford, UK, Blackwell Publishing, 274 p.

Bürgmann, R., Kogan, M.G., Steblov, G.M., Hilley, G., Levin, V.E., and Apel, E., 2005, Interseismic coupling and asperity distribution along the Kamchatka subduction zone: Journal of Geophysical Research, v. 110, B07405, doi:10.1029/2005JB003648.

Carver, G., Jayko, A.S., Valentine, D.W., and Li, W.H., 1994, Coastal uplift associated with the 1992 Cape Mendocino earthquake, northern California: Geology, v. 22, p. 195–198, doi:10.1130/0091-7613(1994)022<0195:CUAWTC>2.3.CO;2.

Chappell, J., Ota, Y., and Campbell, C., 1998, Decoupling post-glacial tectonism and eustasy at Huon Peninsula, Papua New Guinea, *in* Stewart, I.S., and Vita-Finzi, C., eds., Coastal Tectonics: Geological Society of London Special Publication 146, p. 31–40.

Chen, Y.-G., and Liu, T.-K., 2000, Holocene uplift and subsidence along an active tectonic margin southwestern Taiwan: Quaternary Science Reviews, v. 19, p. 923–930, doi:10.1016/S0277-3791(99)00076-1.

Cormier, V.F., 1975, Tectonics near the junction of the Aleutian and Kuril-Kamchatka arcs and a mechanism for middle Tertiary magmatism in the Kamchatka basin: Geological Society of America Bulletin, v. 86, p. 443–453, doi:10.1130/0016-7606(1975)86<443:TNTJOT>2.0.CO;2.

Cross, R.S., and Freymueller, J.T., 2008, Evidence for and implications of a Bering plate based on geodetic measurements from the Aleutians and western Alaska: Journal of Geophysical Research, v. 113, B07405, doi:10.1029/2007JB005136.

Douglas, B.C., Kearney, M.S., and Leatherman, S.P., eds., 2001, Sea Level Rise: History and Consequences: San Diego, California, Academic Press, 232 p.

Erlikh, E.N., Melekestsev, I.V., and Shantser, A.E., 1974, Neotectonics, *in* Luchitskiy, J.V., ed., Kamchatka, Kuril and Kommander Islands: Moscow, Nauka, p. 345–368 (in Russian).

Fedorenko, S.I., 1965, Marine terrace on East Kamchatka coast: MOIP (Moscow Naturalists Society) Geological Department Bulletin, v. XL, no. 4, p. 80–90 (in Russian).

Fedotov, S.A., Gusev, A.A., Shumilina, L.S., and Chernishova, G.V., 1985, The seismofocal zone of Kamchatka: Journal of Volcanology and Seismology, v. 4, p. 91–107.

Freitag, R., Gaedicke, C., Baranov, B., and Tsukanov, N., 2001, Collisional processes at the junction of the Aleutian-Kamchatka arcs: New evidence from fission track analysis and field observations: Terra Nova, v. 13, p. 433–442, doi:10.1046/j.1365-3121.2001.00375.x.

Gaedicke, C., Baranov, B., Seliverstov, N., Alexeiev, D., Tsukanov, N., and Freitag, R., 2000, Structure of an active arc-continent collision area: The Aleutian–Kamchatka junction: Tectonophysics, v. 325, p. 63–85, doi:10.1016/S0040-1951(00)00131-1.

Gardner, T.W., Jorgensen, D.W., Shuman, C., and Lemieux, C.R., 1987, Geomorphic and tectonic process rates: Effects of measured time interval: Geology, v. 15, p. 259–261, doi:10.1130/0091-7613(1987)15<259:GATPRE>2.0.CO;2.

Gehrels, R., 2010, Sea-level changes since the Last Glacial Maximum: An appraisal of the IPCC Fourth Assessment Report: Journal of Quaternary Science, v. 25, p. 26–38, doi:10.1002/jqs.1273.

Geist, E.L., and Scholl, D.W., 1994, Large-scale deformation related to the collision of the Aleutian arc with Kamchatka: Tectonics, v. 13, p. 538–560, doi:10.1029/94TC00428.

Geist, E.L., Titov, V.V., and Synolakis, C.E., 2006, Tsunami: Wave of change: Scientific American, v. 58, p. 56–63.

Gorbatov, A., Kostoglodov, V., Suares, G., and Gordeev, E., 1997, Seismicity and structure of the Kamchatka subduction zone: Journal of Geophysical Research, v. 102, p. 17,883–17,898, doi:10.1029/96JB03491.

Gordeev, E.I., Gusev, A.A., Levina, V.I., Leonov, V.L., and Chebrov, V.N., 2006, Shallow earthquakes in the Kamchatka Peninsula: Journal of Volcanology and Seismology, v. 3, p. 40–55.

Gusev, A.A., and Zobin, V.M., 1975, Macroseismic descriptions of Ust-Kamchatsky earthquake, *in* Fedotov, S.A., ed., Strong Kamchatka Earthquakes in 1971: Vladivostok, Far East Scientific Center of Academy of Science of USSR, p. 85–97 (in Russian).

Hsieh, M.-L., Liew, P.-M., and Hsu, M.-Y., 2004, Holocene tectonic uplift on the Hua-tung coast, eastern Taiwan: Quaternary International, v. 115–116, p. 47–70, doi:10.1016/S1040-6182(03)00096-X.

Huang, W.-J., Johnson, K.M., Fukuda, J., and Yu, S.-B., 2010, Insights into active tectonics of eastern Taiwan from analyses of geodetic and geologic data: Journal of Geophysical Research, v. 115, B03413, doi:10.1029/2008JB006208.

Keller, E.A., and Pinter, N., 2002, Active Tectonics: Earthquakes, Uplift, and Landscape (2nd ed.): Upper Saddle River, New Jersey, Prentice-Hall, 350p.

Kirienko, A.P., and Zolotarskaya, C.B., 1989, Some patterns of the Earth surface deformation of eastern Kamchatka during the period 1966–1983: Journal of Volcanology and Seismology, v. 2, p. 80–93.

Kogan, M.G., and Steblov, G.M., 2008, Current global plate kinematics from GPS, 1995–2007, with the plate-consistent reference frame: Journal of Geophysical Research, v. 113, B04416, doi:10.1029/2007JB005353.

Kozhurin, A.I., 1985, Quaternary tectonics of the Kumroch Range and the Kamchatsky Peninsula, eastern Kamchatka: Geotectonica, v. 2, p. 76–87.

Kozhurin A.I., 1990, Recent strike-slip faults in the Kumroch Range and Kamchatsky peninsula area, eastern Kamchatka: Tikhookeanskaya Geologiya, v. 6, p. 45–55 (in Russian).

Kozhurin, A.I., 2004, Active faulting at the Eurasian, North American and Pacific plates junction: Tectonophysics, v. 380, p. 273–285, doi:10.1016/j.tecto.2003.09.024.

Kozhurin, A.I., 2007, Active faulting in the Kamchatsky Peninsula, Kamchatka-Aleutian junction, *in* Eichelberger, J., Gordeev, E., Kasahara, M., Izbekov, P., and Lees, J., eds., Volcanism and Subduction: The Kamchatka Region: American Geophysical Union Geophysical Monograph 172, p. 263–282.

Kozhurin, A.I., 2009, A dangling slab and arc-normal extension: The case of Kamchatka, Russia: Eos (Transactions, American Geophysical Union), v. 90, Fall Meeting supplement, abstract T41C–2034.

Kozhurin, A., 2012, Active faulting of Russian Far East: 1st Workshop on Fundamental and Applied Problems of Russian Tsunami Warning System: Novosibirsk, Russia, http://conf.nsc.ru/RTWS-2012/ru/participationview/120141 (last accessed 26 June 2013).

Kozhurin, A., and Pinegina, T., 2011, Active faulting in the Kamchatsky Peninsula as evidence for the Kamchatka-Aleutian collision: 7th Biannual Workshop on Japan-Kamchatka-Alaska Subduction Processes, JKASP-2011 (extended abstract): Petropavlovsk-Kamchatsky, Russia, p. 125–128, http://www.kscnet.ru/ivs/slsecret/jkasp_2011/abstr/abs57.pdf (last accessed 25 June 2013).

Lajoie, K.R., 1986, Coastal tectonics, *in* Wallace R., panel chairman, Active Tectonics: Washington, D.C., National Academy Press, Studies in Geophysics Series, Geophysics Research Forum, p. 95–117.

Lander, A.V., and Pinegina, T.K., 2010, Paradoxes of the Olyutorsky earthquake source—Underlying structure and dynamics, *in* Chebrov, V.N., ed., Proceedings of the Second Regional Scientific and Technical Conference “Problems of integrated Geophysical Monitoring of the Russian Far East”: Petropavlovsk-Kamchatsky, Geophysical Survey RAS, p. 131–136 (in Russian).

Lander, A.V., and Shapiro, M.N., 2007, The origin of the modern Kamchatka subduction zone, *in* Eichelberger, J., Gordeev, E., Kasahara, M., Izbekov, P., and Lees, J., eds., Volcanism and Subduction: The Kamchatka Region: American Geophysical Union Geophysical Monograph 172, p. 56–64.

Lander, A.V., Bukchin, B.G., Kiryushin, A.V., and Droznin, D.V., 1996, The tectonic environment and source parameters of the Khailino, Koryakiya earthquake of March 8, 1991: Does a Beringia plate exist?: Computational Seismology and Geodynamics (translated version by American Geophysical Union), v. 3, p. 80–96.

Levin, V.E., 2009, GPS monitoring of recent crustal movements in Kamchatka and the Commander Islands during 1997–2007: Journal of Volcanology and Seismology, v. 3, p. 200–209, doi:10.1134/S0742046309030063 (in Russian, English translation).

Levin, V.E., Gordeev, E.I., Bakhtiarov, V.F., and Kasahara, M., 2002, Preliminary results from GPS monitoring in Kamchatka and the Komandorskie Islands: Journal of Volcanology and Seismology, v. 1, p. 3–11.

Levin, V.E., Maguskin, M.A., Bakhtiarov, V.F., Pavlov, V.M., and Titkov, N.N., 2006, Multisystem geodetic monitoring of recent crustal movements in Kamchatka and the Commander Islands: Journal of Volcanology and Seismology, v. 3, p. 54–68.

Litchfield, N., Wilson, K., Berryman, K., and Wallace, L., 2010, Coastal uplift mechanisms at Pakarae River mouth: Constraints from a combined Holocene fluvial

[2]“Vestnik KRAUNTS Nauki o zemle” also translated as *Bulletin of Kamchatka Regional Association “Educational-Scientific Center” Earth Sciences.*

and marine terrace dataset: Marine Geology, v. 270, p. 72–83, doi:10.1016/j.margeo.2009.10.003.

Mackey, K.G., Fujita, K., Gunbina, L., Kovalev, V., Imaev, V., and Kozmin, B., 1997, Seismicity of the Bering Strait region: Evidence for a Bering block: Geology, v. 25, p. 979–982, doi:10.1130/0091-7613(1997)025<0979:SOTBSR>2.3.CO;2.

Mackey, K.G., Fujita, K., Hartse, H.E., Stead, R.J., Steck, L.K., Gunbina, L.V., Leyshuk, N., Shibaev, S.V., Koz'min, B.M., Imaev, V.S., Gordeev, E.I., Chebrov, V.N., Masal'ski, O.K., Gileva, N.A., Bormatov, V.A., Voitenok, A.A., Levin, Y.N., and Fokina, T.A., 2010, Seismicity map of eastern Russia, 1960–2010: Seismological Research Letters, v. 81, p. 761–768, doi:10.1785/gssrl.81.5.761.

Markovskiy, B.A., Seliverstova, R.A., and Lobov, V.M., 1989, State Geological Map of the USSR: New Series, Sheets O-57, 58: Leningrad VSEGEI, scale 1:100,000 (in Russian).

Martin, M.E., Bourgeois, J., Pinegina, T.K., and Kravchunovskaya, E.A., 2004, Geomorphology of beach ridges and Holocene terraces on Kamchatka: A complex interplay of tectonics, volcanism and coastal processes: Eos (Transactions, American Geophysical Union), v. 85, no. 47, Fall Meeting supplement, abstract H51C–1145.

Martin, M.E., Weiss, R., Bourgeois, J., Pinegina, T.K., Houston, H., and Titov, V.V., 2008, Combining constraints from tsunami modeling and sedimentology to untangle the 1969 Ozernoi and 1971 Kamchatskii tsunamis: Geophysical Research Letters, v. 35, L01610, doi:10.1029/2007GL032349.

McElfresh, S.B.Z., Harbert, W., Ku, C.-Y., and Lin, J.-S., 2002, Stress modeling of tectonic blocks at Cape Kamchatka, Russia, using principal stress proxies from high-resolution SAR: New evidence for the Komandorskiy block: Tectonophysics, v. 354, p. 239–256, doi:10.1016/S0040-1951(02)00341-4.

McSaveney, M.J., Graham, I.J., Begg, J.G., Beu, A.G., Hull, A.G., Kim, K., and Zondervan, A., 2006, Late Holocene uplift of beach ridges at Turakirae Head, south Wellington coast, New Zealand: New Zealand Journal of Geology and Geophysics, v. 49, no. 3, p. 337–358, doi:10.1080/00288306.2006.9515172.

Merritts, D., 1996, The Mendocino triple junction: Active faults, episodic coastal emergence, and rapid uplift: Journal of Geophysical Research, v. 101, p. 6051–6070, doi:10.1029/95JB01816.

Merritts, D., Eby, R., Harris, R., Lawrence, E., and Chang, H., 1998, Variable rates of late Quaternary surface uplift along the Banda Arc–Australian plate collision zone, eastern Indonesia, *in* Stewart, I.S., and Vita-Finzi, C., eds., Coastal Tectonics: Geological Society of London Special Publication 146, p. 213–224.

Meyers, R.A., Smith, D.G., Jol, H.M., and Peterson, C.D., 1996, Evidence for eight great earthquake-subsidence events detected with ground penetrating radar, Willapa Barrier, Washington: Geology, v. 24, p. 99–102, doi:10.1130/0091-7613(1996)024<0099:EFEGES>2.3.CO;2.

Nelson, A.R., and Manley, W.F., 1992, Holocene coseismic and aseismic uplift of Isla Mocha, south-central Chile: Quaternary International, v. 15/16, p. 61–76, doi:10.1016/1040-6182(92)90036-2.

Okal, E.A., and Talandier, J., 1986, T-wave duration, magnitudes and seismic moment of an earthquake-application to tsunami warning: Journal of Physics of the Earth, v. 34, p. 19–42, doi:10.4294/jpe1952.34.19.

Ota, Y., and Yamaguchi, M., 2004, Holocene coastal uplift in the western Pacific Rim in the context of late Quaternary uplift: Quaternary International, v. 120, p. 105–117, doi:10.1016/j.quaint.2004.01.010.

Park, J., Levin, V., Brandon, M., Lees, J., Peyton, V., Gordeev, E., and Ozerov, A., 2002, A dangling slab, amplified arc volcanism, mantle flow and seismic anisotropy in the Kamchatka plate corner, *in* Stein, S., and Freymueller, J.T., eds., Plate Boundary Zones: American Geophysical Union Geodynamics Monograph 30, p. 295–324.

Pedoja, K., Bourgeois, J., Pinegina, T., and Higman, B., 2006, Does Kamchatka belong to North America? An extruding Okhotsk block suggested by coastal neotectonics of the Ozernoi Peninsula, Kamchatka, Russia: Geology, v. 34, p. 353–356, doi:10.1130/G22062.1.

Pedoja, K., Husson, L., Regard, V., Cobbold, R.P., Ostanciaux, E., Johnson, M.E., Kershaw, S., Saillard, M., Martinod, J., Furgerot, L., Weill, P., and Delcaillau, B., 2011, Relative sea-level fall since the last interglacial stage: Are coasts uplifting worldwide?: Earth-Science Reviews, v. 108, p. 1–15, doi:10.1016/j.earscirev.2011.05.002.

Pedoja, K., Authemayou, C., and Pinegina, T., Bourgeois, J., Nexer, M., Bernard Delcaillau, B., and Regard, V., 2013, "Arc-continent collision" of the Aleutian-Komandorsky arc into Kamchatka: Insight into Quaternary tectonic segmentation through Pleistocene marine terraces and morphometric analysis of fluvial drainage: Tectonics, doi:10.1002/tect.20051 (in press).

Peltier, W.R., 2002, On eustatic sea level history: Last Glacial Maximum to Holocene: Quaternary Science Reviews, v. 21, p. 377–396, doi:10.1016/S0277-3791(01)00084-1.

Pevzner, M.M., Ponomareva, V.V., and Melekestsev, I.V., 1997 (1998), Chernyi Yar—Reference section of the Holocene ash markers at the northeastern coast of Kamchatka: Volcanology and Seismology, v. 19, p. 389–406 (translated from Pevzner et al., 1997).

Pflanz, D., Gaedicke, C., Freitag, R., Krbetschek, M., Tsukanov, N., and Baranov, B., 2013, Neotectonics and recent uplift at Kamchatka and Aleutian arc junction, Kamchatka Cape area, NE Russia: International Journal of Earth Sciences, v. 102, p. 903–916, doi:10.1007/s00531-012-0830-z.

Pinegina, T.K., Bourgeois, J., Bazanova, L.I., Braitseva, O.A., and Egorov, Yu.O., 2002, Tsunami deposits and analysis of tsunami risk at Khalatyrka beach, region of Petropavlovsk-Kamchatsky, Pacific coast of Kamchatka, Russia, *in* Levin, B.W., and Nosov, M.A., eds., Proceedings of the International Workshop "Local Tsunami Warning and Mitigation": Petropavlovsk-Kamchatsky: Moscow, Russia, Janus-K., p. 122–131 (in English).

Pinegina, T., Bourgeois, J., Bazanova, L., Melekestsev, I., and Braitseva, O., 2003, Millennial-scale record of Holocene tsunamis on the Kronotskiy Bay coast, Kamchatka, Russia: Quaternary Research, v. 59, p. 36–47, doi:10.1016/S0033-5894(02)00009-1.

Pinegina, T.K., Kravchunovskaya, E.A., Lander, A.V., Kozhurin, A.I., Bourgeois, J., and Martin, M.E., 2010, Holocene vertical movement of Kamchatsky Peninsula coast, Kamchatka, based on studies of marine terraces: Vestnik KRAUNTS Nauki o zemle, v. 15, p. 231–247 (in Russian) (see footnote 2).

Pinegina, T.K., Kozhurin, A.I., and Ponomareva, V.V., 2012, Seismic and tsunami hazard for the Ust-Kamchatsk village, Kamchatka, from paleoseismological investigations: Vestnik KRAUNTS Nauki o zemle, v. 19, p. 7–28 (in Russian). (see footnote 2)

Ponomareva, V.V., Kyle, P.R., Pevzner, M.M., Sulerzhitsky, L.D., and Hartman, M., 2007, Holocene eruptive history of Shiveluch volcano, Kamchatka Peninsula, *in* Eichelberger, J., Gordeev, E., Kasahara, M., Izbekov, P., and Lees, J., eds., Volcanism and Subduction: The Kamchatka Region: American Geophysical Union Geophysical Monograph 172, p. 263–282.

Portnyagin, M., Hoernle, K., Avdeiko, G., Hauff, F., Werner, R., Bindeman, I., Uspensky, V., and Garbe-Schönberg, D., 2005, Transition from arc to oceanic magmatism at the Kamchatka-Aleutian junction: Geology, v. 33, p. 25–28, doi:10.1130/G20853.1.

Reimer, P.J., Baillie, M.G.L., Bard, E., Bayliss, A., Beck, J.W., Blackwell, P.G., Bronk Ramsey, C., Buck, C.E., Burr, G.S., Edwards, R.L., Friedrich, M., Grootes, P.M., Guilderson, T.P., Hajdas, I., Heaton, T.J., Hogg, A.G., Hughen, K.A., Kaiser, K.F., Kromer, B., McCormac, F.G., Manning, S.W., Reimer, R.W., Richards, D.A., Southon, J.R., Talamo, S., Turney, C.S.M., van der Plicht, J., and Weyhenmeyer, C.E., 2009, IntCal09 and Marine09 radiocarbon age calibration curves, 0–50,000 years cal BP: Radiocarbon, v. 51, p. 1111–1150.

Saltonstall, P., and Carver, G.A., 2002, Earthquakes, subsidence, prehistoric site attrition and the archaeological record: A view from the Settlement Point site, Kodiak Archipelago, Alaska, *in* Torrence, R., and Grattan, J., eds., Natural Disasters and Cultural Change: One World Archaeology Series Volume 45: London, Routledge, p. 172–191.

Scholl, D.W., 2007, Viewing the tectonic evolution of the Kamchatka-Aleutian, KAT, connection with an Alaska crustal extrusion perspective, *in* Eichelberger, J., Gordeev, E., Kasahara, M., Izbekov, P., and Lees, J., eds., Volcanism and Subduction: The Kamchatka Region: American Geophysical Union Geophysical Monograph 172, p. 3–35.

Selivanov, A.O., 1996a, Morphological changes on Russian coasts under rapid sea-level changes: Examples from the Holocene history and implications for the future: Journal of Coastal Research, v. 12, p. 823–830.

Selivanov, A.O., 1996b, Global Sea-Level Change in the Pleistocene-Holocene and the Development of Ocean Shorelines: Moscow, Water Problems Institute, Russian Academy of Science, 268 p. (in Russian).

Seliverstov, N.I., 1998, The Bottom Structure near East Kamchatka and Geodynamics of the Junction Zone of the Kuril-Kamchatka and Aleutian Island Arcs: Moscow, Scientific World, 164 p.

Seliverstov, N.I., 2009, Geodynamical Zonation of the Kuril-Kamchatka and Aleutian Island Arc: Petropavlosk-Kamchatsky, Russian Academy of Science, 191 p. (in Russian).

Shennan, I., Long, A.J., Rutherford, M.M., Innes, J.B., Green, F.M., Kirby, J.R., and Walker, K.J., 1998, Tidal marsh stratigraphy, sea-level change and large earthquakes II: Submergence events during the last 3500 years at Netarts Bay, Oregon, USA: Quaternary Science Reviews, v. 17, p. 365–393, doi:10.1016/S0277-3791(97)00055-3.

Sugihara, K., Nakamori, T., Iryu, Y., Sasaki, K., and Blanchon, P., 2003, Holocene sea-level change and tectonic uplift deduced from raised reef terraces, Kikai-jima, Ryukyu Islands, Japan: Sedimentary Geology, v. 159, p. 5–25, doi:10.1016/S0037-0738(03)00092-7.

Tamura, T., Murakami, F., and Watanabe, K., 2010, Holocene beach deposits for assessing coastal uplift of the northeastern Boso Peninsula, Pacific coast of Japan: Quaternary Research, v. 74, p. 227–234, doi:10.1016/j.yqres.2010.07.009.

Vita-Finzi, C., and Situmorang, B., 1989, Holocene coastal deformation in Simeulue and Nias, Indonesia: Marine Geology, v. 89, p. 153–161, doi:10.1016/0025-3227(89)90031-5.

Wilson, K., Berryman, K., Litchfield, N., and Little, T., 2006, A revision of mid-late Holocene marine terrace distribution and chronology at the Pakarae River mouth, North Island, New Zealand: New Zealand Journal of Geology and Geophysics, v. 49, p. 477–489, doi:10.1080/00288306.2006.9515182.

Woodroffe, S.A., and Horton, B.P., 2005, Holocene sea-level changes in the Indo-Pacific: Journal of Asian Earth Sciences, v. 25, p. 29–43, doi:10.1016/j.jseaes.2004.01.009.

Yamaguchi, M., and Ota, Y., 2002, Tectonic and paleoseismological significance of Holocene marine terraces on the east coast of Coastal Range, Taiwan: Journal of Geography Chigaku-zasshi, v. 111, p. 323–340, doi:10.5026/jgeography.111.3_323.

Science Editor: Jon Pelletier
Associate Editor: Nancy Riggs

Manuscript Received 13 September 2012
Revised Manuscript Received 6 May 2013
Manuscript Accepted 1 July 2013

Printed in the USA